CHALMERS

Impact on the East Ormo tower's stability due to the increase in wind load

Master of Science Thesis in Geo and Water Engineering

ADNAN DROBIĆ

Department of Civil and Environmental Engineering
Division of GeoEngineering

Geotechnical Engineering Research Group

CHALMERS UNIVERSITY OF TECHNOLOGY
Göteborg, Sweden 2011

Master's Thesis 2011:05

MASTER'S THESIS 2011:05

Impact on the East Ormo tower's stability due to the increase in wind load

Master of Science Thesis in Geo and Water Engineering

ADNAN DROBIĆ

Supervisors:

Andreas Åberg and Peter Wilén, Vattenfall Power Consult

Claes Alén, Chalmers University of Technology

Department of Civil and Environmental Engineering
Division of GeoEngineeringGeotechnical Engineering Research GroupCHALMERS UNIVERSITY OF TECHNOLOGY

Göteborg, Sweden 2011

Impact on the East Ormo tower's stability due to the increase in wind load

Master of Science Thesis in Geo and Water Engineering

ADNAN DROBIĆ

Examensarbete / Institutionen för bygg- och miljöteknik,
Chalmers tekniska högskola 2011:05

Department of Civil and Environmental Engineering
Division of GeoEngineeringGeotechnical Engineering Research GroupChalmers University of Technology
SE-412 96 Göteborg
Sweden
Telephone: + 46 (0)31-772 1000

Cover:
The East Ormo Tower

Chalmers Reproservice / Department of Civil and Environmental Engineering
Göteborg, Sweden 2011

Impact on the East Ormo tower's stability due to the increase in wind load

Master of Science Thesis in Geo and Water Engineering

ADNAN DROBIĆ
Department of Civil and Environmental Engineering
Division of GeoEngineeringGeotechnical Engineering Research GroupChalmers University of Technology

ABSTRACT

Concern over the large filling being built in conjunction with Ormos eastern tower has long been an issue on Waterfall Consulting. The pressure from the filling together with an increasing wind speed due to climate change can be decisive factor leading to the tower's collapse. The East Tower has been subjected to lateral load from embankment since 1998.

The Ormo screen plant is located in the Nordre River, just a few hundred meters downstream from branching point with Göta River. The primary objective is to increase the flow of the Göta River when this is under 300 m^3/s. This is achieved by the four big screens which are raised and dams up the flow of Nordre River leading that the flow increases in the Göta River. Thereby reducing the risk for sea water intrusion into the water production plant for city of Gothenburg during the low water flow.

This master thesis has studied the increase in wind load, impact on the tower's stability, together with other permanent and variable loads. Because wind load can be charged to the tower from all directions, the project also analyzed the wind pressure from the dominant wind directions in the region. The characteristic load and the corresponding design load is calculated using partial factor of safety. The stability of tower has been calculated for ultimate limit state. Consequences of these loads are deformations of piles and tower's foundation. The project deals with stability of soil as well. These analyses are done by Slide 2D computer program.

The main issue was to calculate the internal forces caused by loads on the piles using the Rymdpålgrupp computer program. The value of cross-sectional forces is compared with the value of total capacity for the most loaded pile.

Additional studies need to be made in order to give information of timber durability. The timber piles are usually exposed to both biologic and chemical attack that plays a crucial role of piles stability.

Key words: Lateral earth pressure, wind load, pile foundation, undrained shear strength, structural failure, pile cap, cross-sectional forces, ultimate limit state design, partial factors.

Contents

Preface

This Master thesis project has been accomplished at Chalmers University of Technology, in the department of Civil and Environmental Engineering, division of Geo Engineering and in cooperation with Infrastructure and Civil Engineering department of Vattenfall.

The project has been initiated by Andreas Åberg and Peter Wilén from Vattenfall Power Consultant AB.

In this project the stability of East Ormo Tower has been investigated. The tower is located at the Nordre River and it has been subjected to lateral pressure from a newly built embankment. The filling is laid on the east side of the tower and together with the strong east winds may cause the tower to collapse.

Göteborg February 20011

Adnan Drobić

Acknowledgements

Thanks to Andreas Åberg at Vattenfall Power Consultant AB, which came with the proposal for this thesis, which also come with all the help and support when it was needed most.

Thanks to my examiner professor Claes Alén at the department of Civil and Environmental Engineering for all understanding of changing plans during the project.

I would like to express my deepest gratitude to Sigmund and Veino on Software Engineering Company in Gothenburg. Without their help and software, I would not be able to implement this project and come to these conclusions.

Also much gratitude to Kenneth Häggkvist and Magnus Asp at SMHI who had time and answered all my questions.

Notations

Roman upper case letters

A - Cross-sectional area [m^2]

Cdyn - Gust factor [-]

$C_{exp}(z)$ - Exposure factor [-]

Cpe-Pressure coefficient for the external pressure

E - Modulus of elasticity [kPa]

Fs - Factor of safety

Fk - Breaking load [kN]

K_A - Lateral earth pressure coefficient [-]

Kv - Torsional factor [m^4]

Lp - Pile length [m^2]

Mx, My, Mz - Bending moment [kNm]

N - Normal force [kN]

Pw - Water pressure [kN/m^2]

Px,Py,Pz - Point load [kN]

Pa - Lateral earth pressure [kN/m^2]

R - Load capacity

Rd - Design load capacity

S - Load effect

V - Shear force [kN]

Z(e) - Reference height for the external pressure

Z_{min} - Minimum height[m]

Zo – Roughness length

Wk - Characteristic wind load [kN]

We – Wind pressure on the external surfaces [kN]

Roman lower case letters

b -Width [m]

bm -Foundation modulus [MN/m^3]

$c_e(z)$-Exposure factor

c_f - Shear strength [kPa]

c_u - Undrained shear strength [kPa]

d - Depth of the structure [m]

dp - Pile diameter [m]

f - Material strength

fd - Design value on a material strength

f_k - Characteristic value of strength

h - Hight of tower above water level [m]

he - Height of the embankment (m)

kd - Subgrade reaction coefficient [MN/m^2]

q_b- Basic velocity pressure [kN]

q_d - Design load [kN]

q_k - Characteristic velocity pressure [kN/m^2]

$q_p(Ze)$- Peak velocity pressure [kN/m^2]

q_{ref} - Reference velocity pressure [kN/m^2]

v - Wind speed [m/s]

v_{ref} - Reference value for wind speed [m/s]

v_b -basic wind velocity[m/s]

z -Height or depth from water level [m]

Greek letters

β - *Terrain factor [-]*

γ - *Unit weight [kN/m^3]*

γ_f - *Partial factor for load*

γ_m - *Partial factor for a material property*

γ_n - *Partial factor for safety class*

γ_w - *Unit weight of water [kN/m^3]*

ρ - *Density [kg/m^3]*

μ - *Form factor*

ϕ - *Angle of internal friction of the material*

υ - *Poisson's ratio [-]*

θ - *Wind direction [°]*

τ - *Shear stress [kPa]*

Abbreviation

BKR- Swedish building design guidelines

BSV 97- Swedish Building Administration handbook of snow and wind loads

SGI - Swedish Geotechnical institute

SMHI - Swedish Meteorological and Hydrological Institute

EW-east-west direction

SN-south-north direction

ww - windward

lw - leeward

1. Introduction

1.1 Background

In connection with the regulation of Lake Vänern in Sweden water barrier structure such as the Ormo screen facility have been built. The plant went into operation 1934th. Main function of this plant is the prevention of intrusion of seawater in to Göta River, which is used for production of fresh water in Gothenburg and the neighboring towns. Figure 1.1 shows the map of southwest Sweden with the city of Gothenburg.

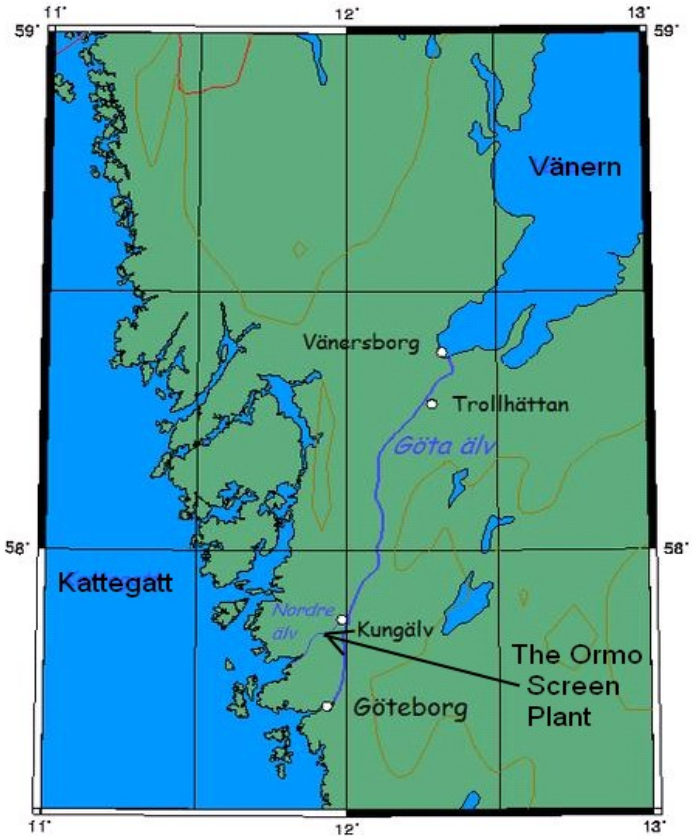

Figure 1.1 Site map of Ormo Screen Plant

Göta River is 93 km long river and flows from Lake Vänern to Älvsborgs fjord in the Kattegat. The average water flow at the mouth is approximately 570 m^3/s with a maximum flow of about 1 030 m^3/s. The River drains Lake Vänern in to Kattegatt at the city of Gothenburg, on the west coast of Sweden.

As shown in the figure above at Kungälv town, the river splits into two, with the northern part being the Nordre River and the southern part keeping the same name Göta River where the fresh water intake for Gothenburg is located just some kilometers downstream of the branching point.

At Trollhättan and Lilla Edet, downstream of Lake Vänern, there are dams for hydropower purpose and the dams regulate the flow of Göta River. If the flow of water in the Göta River is very low, back flow of water from Kattegatt Sea, to both branches of Göta River is inevitable. This back flow of sea water into Göta River has a big impact on the water supply system. To avoid this problem the flow of water in the southern branch should be increase. During period of low flow, to maintain a higher flow in the Göta River, the low in the Nordre River should be restricted. Hence, as located in the figure below, screen regulating structure is constructed on Nordre River, to avoid the intrusion of salt water in to the fresh water production plant. When the screens are open the ¾ of water goes by Nordre River, while if the screens are closed only about ¼ goes this route. Screens are operated from the operations center in Trollhättan as mentioned above. Normally, the screen will be completely above water level when the water flow is 300 m^3/s and less. The Ormo screen plant has two towers as shown on the figure 1.2, which house machineries to maneuver four screens. Each of them is 37 meters long that restrict the water flow of Nordre River. The function of system also shown on Figure 2.2 works by the ropes and wires attached to the counterweight. The counterweight is filled with varying amount of water to balance the variable water pressure on the screen (Forsberg et. al, 2002). The structure is mainly important in summer time, when river discharge is low and sea level is high. The intrusion of seawater in winter is less crucial due to the high discharge of the river and low sea level.

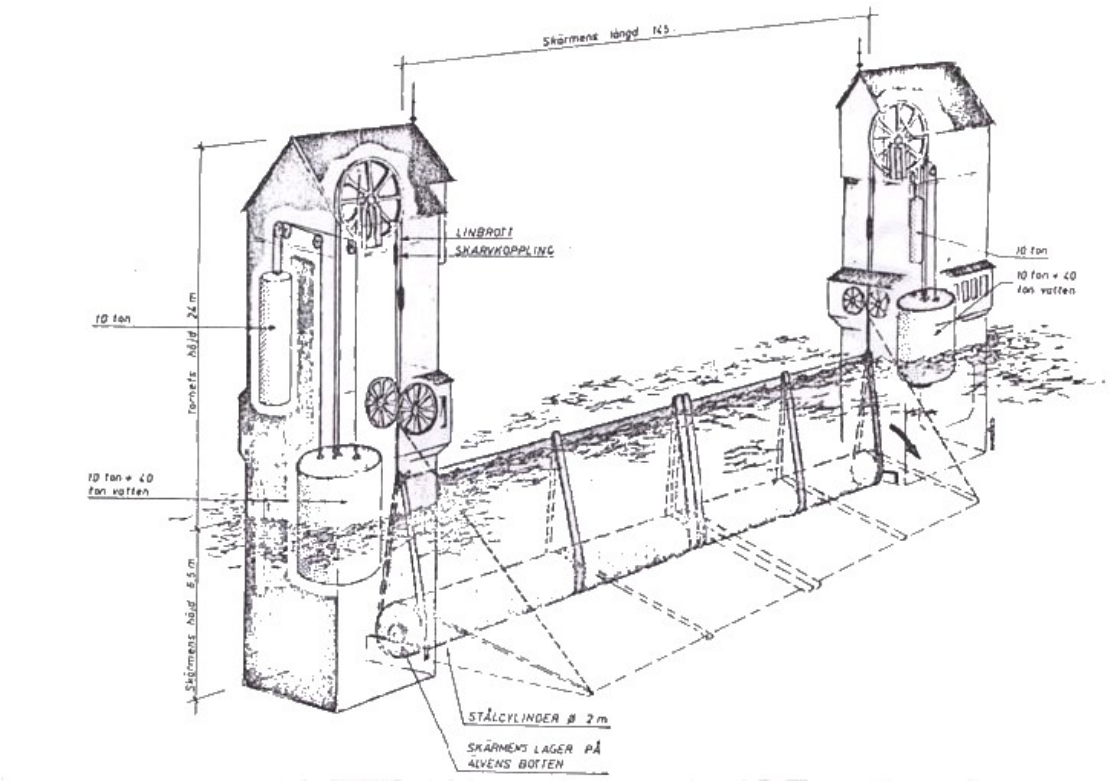

Figure 1.2 Three Dimensional view of Ormo Screen Plant

1.2 Scope

The Ormo plant was built in the 1930's and has been restored in two stages, one in 1950's and the other in 1979's. A condition for both towers has been investigated before. Some measurements and checks have been performed including a safety evaluation by Swedpower in 2002.

Stability of the plant is not the problem under normal circumstances. The ongoing climate change can lead to problem for the east towel.

The Swedish Meteorological and Hydrological Institute (SMHI) have collected data of wind speed in the area which are presented in the appendix VI. It can be conclude that the highest wind speed has increased in the Ormo area since 1950. If increase in wind load adds to the earth pressure from the embankment the whole tower can collapse. Besides the pressure from the embankment there is also a horizontal pressure from the water, which is perpendicular to the pressure from the embankment.

The analyses of those lateral loads acting together with the vertical load of the constructions own weight is the scope of this master thesis.

The Ormo screen plant is provisionally classified as a class A plant, which means that the impact on social functioning due to loss of function of the system would be great Forsberg et. al, 2002).

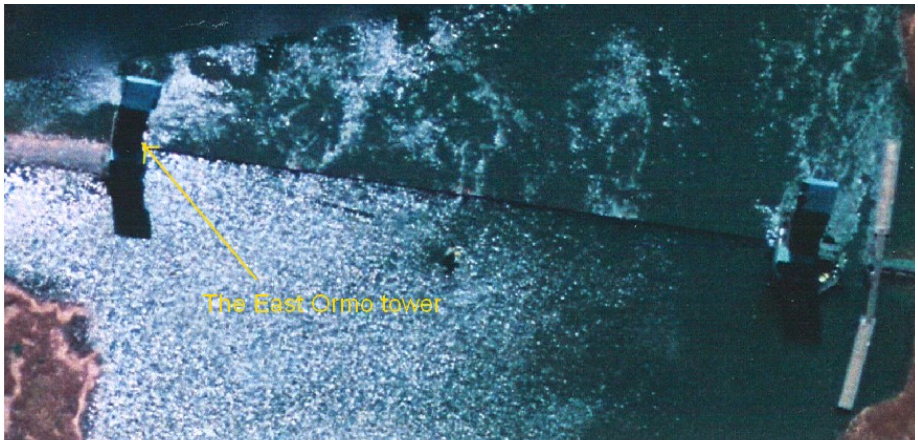

Photo 1 - Ormo's screen facility with damming, downstream view

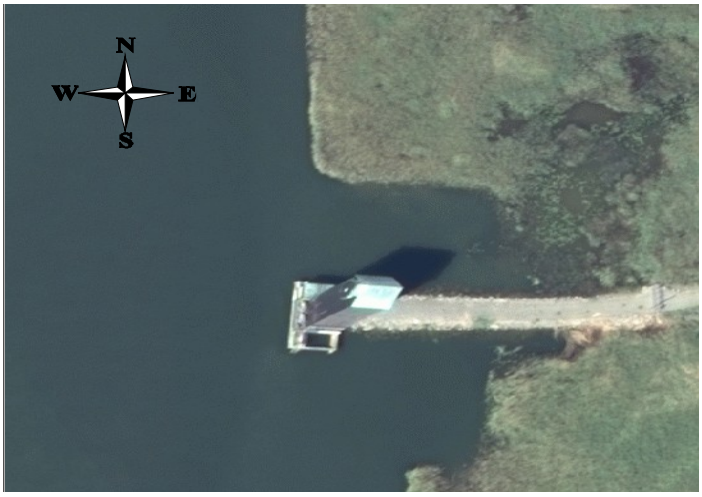

Photo 2 - The East Tower's directions upstream view

1.3 Outline

This study report is divided into eight different parts. The first part is a brief description throughout the study area.

The Chapter 2 presents the Geotechnical and Geological Conditions followed by Chapter 3, which deals with Construction and Geometry of the structure.

In Chapter 4 the soil slope stability has performed assuming that the tower has not any influence on the slip surface.

Partial coefficient method and its factors are described in Chapter 5.

Calculations of action forces such as wind load, earth pressure and water pressure have been performed in Chapter 6.

The results are presented in Chapter 7 as cross-sectional forces for the whole pile group. The calculation of the most loaded pile is done in the same chapter to get to know if resistance is greater than the action or if the deformation is within the permissible limit. The calculation is performed for several wind directions and by using the software called Rymdpålgrupp of Software Engineering Company.

Finally the conclusion of the results is presented in Chapter 8.

2. Geotechnical and Geological Conditions

Characteristic of most Swedish soils is that they are formed during a glacial period. The difference can be made between the soils derived directly from the ice and the soil built from melting water witch is therefore classified as the glacial soils. The East OrmoTower is located on the mighty layers of glacial clay, which also was formed in connection with the ice melting, but in larger formation with more or less stagnant water.

The depth to the rock below the pile cap varies and is between 15 and 25 m. Above the bedrock level is the thinner layer of friction material. The thickness of sand layer varies but can be determined according to appendix I, approximately four meter. Upon the sand layer is the normal consolidated clay deposit with thickness between 15 and 20 meter.

Seismic surveys have been conducted to determine the depth of rock. The bedrock slope under the tower shown in the figure 2.1 increasing towards Hisingen, the area east of the Ormo plant. Influence of slope has been accounted in assessment of piles length. With help of Vattenfall drawing 3-237949 and existing scale the length of each pile was established.

As shown in Figure 2.2, below the pile cap (the depth is measured from the water level) the ground is filled with stone down to a depth of -8, 4 m. The top of the pile cutting plane is located at -7,5 m. Below the stone layer the ground is filled with gravel down to a depth of -12 m. The flow direction of Nordre River as well as the side of tower witch is opposite to embankment is shown on the same figure.

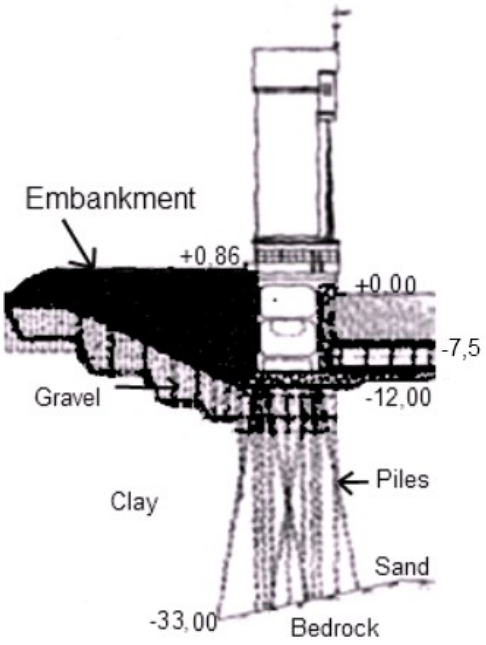

Figure 2.1 The side view of The East Ormo Tower

The geotechnical data for this study does not involve any kind of laboratory testing and are taken from the Rya – Stenungsund pipe-line stability studies report of VBB Viak and SwedPower. Approximate values of the friction angle for friction soils are shown in Table 6.11. Material parameters used in this rapport and foundation of the tower according to data from Vattenfall Consulting are summarized in the table below. The undrained shear strength varied in accordance to equation 4.1.

Table 2.1 Material properties of the soil (Rehnström 2001)

Material	*Unit weight over water table [kN/m3]*	*Unit weight under water table [kN/m3]*	*Friction angle[°]*	*Undrained shear strength, c_u [kPa]*
Stone (Macadam)	*18*	*11*	*35*	-
Gravel	*18*	*11*	*35*	-
Clay	*16*	*6*		*Varied*

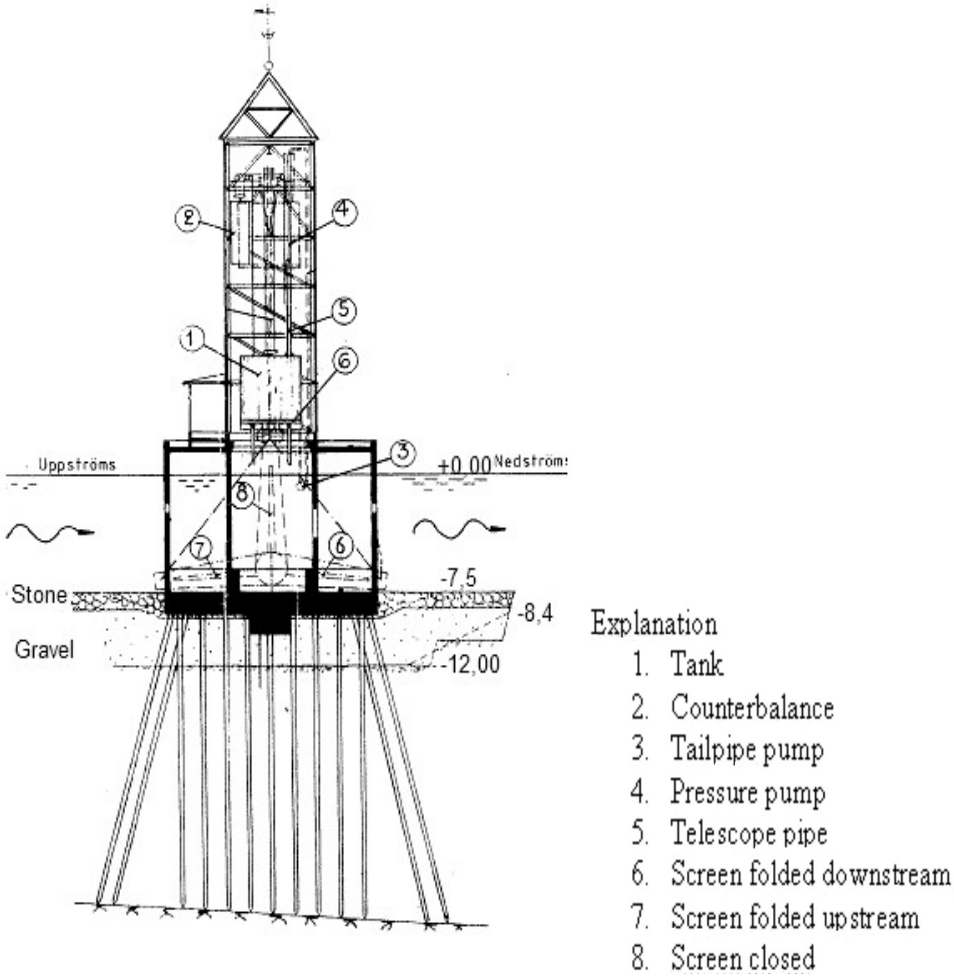

Figure 2.2 The cross sectional view of the structure with the function components

3. Construction and Geometry

The whole construction as shown on Photo 3 below is positioned in the river channel and supported by piles. Before foundation of the plate the trench was dredged and filled with the gravel. The foundation is below the water surface on which caisson of reinforced concrete with towers have been connected.

On the lower edge of the fundament a steel frame was installed for attachment of the bearing bracket to witch the screen consisting of horizontal steel pipe with a fence are connected. The fundament was constructed with a heel in the middle of the bottom plate. Heel with width of 3 m is continuous from edge to edge of the plate and has the task of counter-slip pad.

The caisson is 14 m long, 6 m width and reaches the 2 m above the water level. As sealing both between different ground elements as well as tower and main land a simple sheet pile of wood are installed. The new sheet pile wall of iron 12 m long and 0,076 m thick was wrapped in the middle of the embankment 1998 because the old one was damaged. Distance between them is about 0.5 m.

The supporting frame of tower is welded steel lattice construction. The outside is tower covered with two layers of wood paneling.

The roof is done of wood truss which external is covered by copper sheet. On the upstream side of the tower is a small extension entirely of wood, housing the necessary inspection and control devices. The front view of tower with dimensions in meter is drawn on Figure 3.1

Photo 3 – The East Ormo Tower

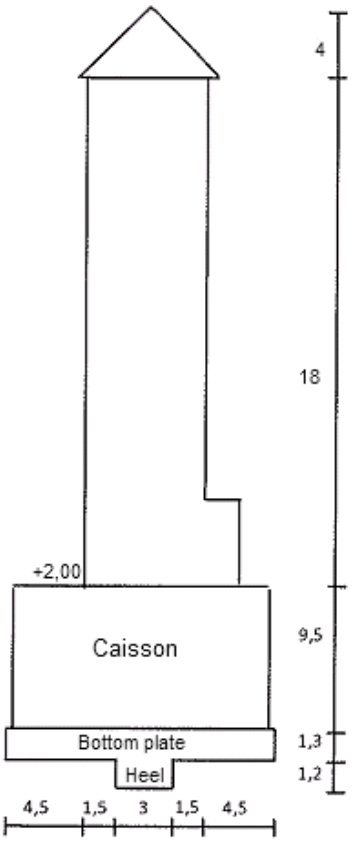

Figure 3.1 Cross section of structure in meters

3.1 Embankment

The embankment was built in 1998, and placed next to the tower caisson wall to access the east tower by foot. The embankment is made of stone with properties as shown in Table 2.1.

The upper part of the embankment is filled with macadam (washed stone product with diameter 32 to 64 mm) up to the +0, 86 m above the water level. Under the macadam laying the less coarse gravel material (Forsberg et al, 2002).

The dimension of the embankment is variable across its length. It is deep close to the tower, approximately 9 m and become shallower far away from the tower. The length is around 57 m. The top width are 4 m right next to the tower, decreasing more and more towards the shoreline probably due to river erosion (hydraulic action). The slope of the embankment corresponds to 1:2.

The majority of the embankment is supported using piles for reasons of stability and settlement.

3.2 Pile Cap

Pile cap is necessary to distribute the load from the super structure to the piles. As shown in Figure 3.2 the pile cap measures 15 in length and 9 meter in width and the thickness is 1.2 meter according to Vattenfall drawing 61922. The pile cap is made out of reinforced concrete and its unit weight is equal to 24 kN/m^3.

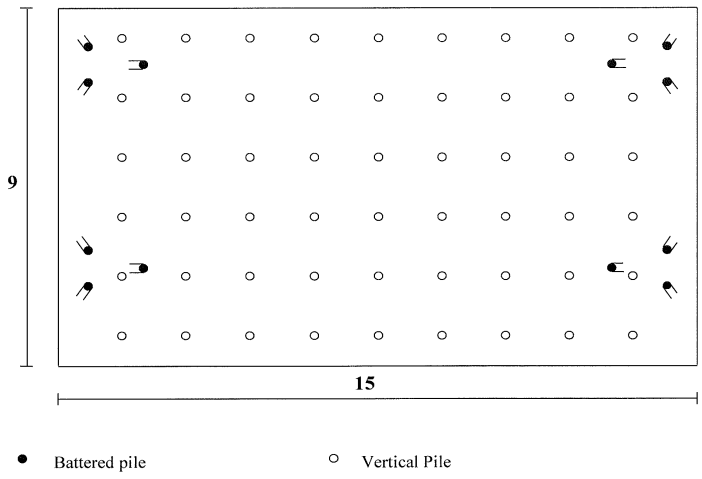

Figure 3.2 The plane view of pile cap

The origin is in the pile cap center. The piles are placed in a rectangularly angled right-oriented coordinate system with x-axis vertical and positive downwards as seen on Figure 7.2.

3.3 Timber Pile Foundation

The tower is supported on a pile foundation, which is composed of two different types of piles, vertical and battered pile. There are 66 piles in total, 12 of which are battered with a slope of 1:4 and the rest are vertical piles.

The depth in which the piles are fixed varied between 18-28 meter according to Vattenfall drawing 4832 measured from the pile cap. The head of the pile is under the water level and it is fixed in the pile cap at -7,5 m. The tip of the piles is rested on bedrock and they are designed as end-bearing piles for the vertical load.

3.3.1 Spacing and configuration between piles

The distance between all piles and their spatial arrangement is shown in Figure 3.3.

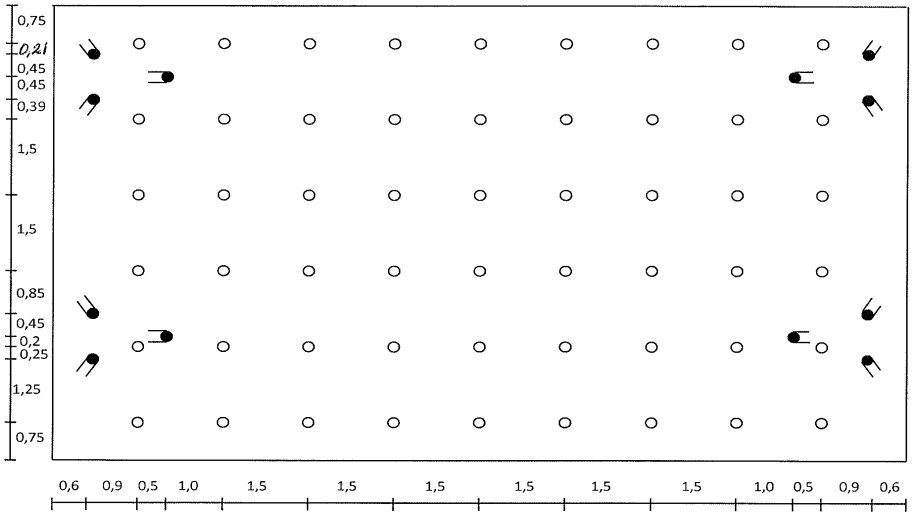

Figure 3.3 Pile cap with distance between piles

Timber piles usually have a varying cross sectional area, which results in different sectional properties and also the end bearing capacity of the pile is highly dependent on the cross sectional area of the tip of the pile. In this pile group all piles are assumed to have the same diameter, which are equal to 7 inches (0.18 m).

The battered piles slope 1:4 is converted into degrees as:

$$\tan\theta = \frac{1}{4} = 14^{\circ}$$

Three dimensional images of all piles are shown in Figure 3.4 below:

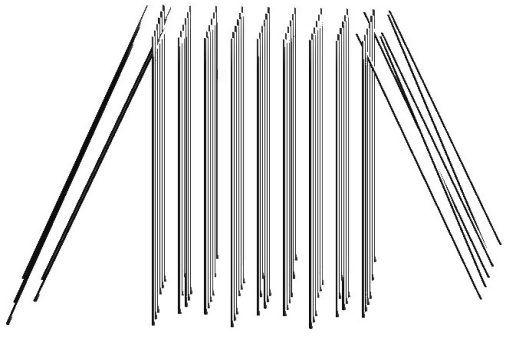

Figure 3.4 Three Dimensional views of piles

4. Soil Slope Stability

The embankment makes a large load on the subsoil of clay. The slippage of the layers can result in additional load with subsequent unwanted impact on the piles and tower.

The analysis of soil slope for Ormo Screen Plant is performed by Slide, 2D limit equilibrium stability software.

4.1 Untrained shear strength

The plenty of boreholes are made at the site during the investigation of pipeline between Rya and Stenungsund. Some of them are few meter while others reach up to 24 m below the ground level. The map with all sites of investigation is shown in Appendix II (SwedPower).

The shear strength measurements have been performed at several locations close to the east tower. The results from borehole BP2520 nearest to Nordre River presented in the rapport Gasledning Rya – Stenungsund, Etapp 1- Rya-Guddeby are chosen. This is because it is located very close to the tower compared to other boreholes and moreover it measure undrained shear strength as deep as 24 m.

Borehole BP2520, is marked in the Appendix II. CPT tests for this borehole are investigated by VBB Viak 1994. The survey shows clay layer with shear strength of 8 kPa at the surface and an increase of 1.2 kPa /m with the depth.

Generally, in the area along the Nordre River clay has a low strength at the top, about 10 kPa, which grows with 1 kPa/m downwards.

The linearly increasing undrained shear strength with depth and under the tower can be written in the form:

$$c_u = c_o + k \cdot z \qquad (4.1)$$

c_o=8 kPa (The shear strength of soil surface)

k = 1,2 [kN/m]

The undrained shear strength for the clay layer at depth of 15 m becomes:

$$c_{uk} = 8 + 1{,}2 \cdot 15 = 26 \text{ kPa}$$

The result above gives the characteristic value. For the ultimate limit state analysis, the design value is required. It is given by equation (4.2).

$$c_{ud} = \frac{c_{uk}}{\gamma_n \cdot \gamma_m} \qquad (4.2)$$

γ_m - Partial factor for a material property

γ_n - Partial factor for safety class

The partial factors for soil parameters are collected in Table 5.1 and used in a computer program.

4.2 Safety Factor

Evaluating the safety factor or probability of failure, for circular or non-circular failure surfaces in soil or rock slopes can easily be calculated by Slide. The program analyzes the stability of slip surfaces using vertical slice limit equilibrium methods. Slide also includes finite element groundwater seepage analysis built right into the program.

In investigations of slopes one often finds that the slip surface has a circular geometry. For our case, the Bishops method is used to calculate the factor of safety or safety against structural failure (*Fs*). The method makes some simplifying assumptions, such as the forces on the side of each slice is horizontal as the sliding mass above the failure surface is divided into a number of slices.

Safety factor is shown with associated grid, above the soil model and is defined as the ratio of average shear strength (c_f) and shear stress (τ).

$$Fs = \frac{c_f}{\tau}$$

The greater the safety factor (Fs) is, the greater safety against structural failure will be. Failure can be expected to occur when Fs ≤1 (Sällförs, 1994).

The soil slope stability has performed assuming that the tower has not any influence on the slip surface because the whole weight of the tower is transferred to the firm bottom.

The soil model was analyzed with the normal water level and shown in Figure 4.1. The safety factor is calculated to be 1,275 which mean that the slope is stable.

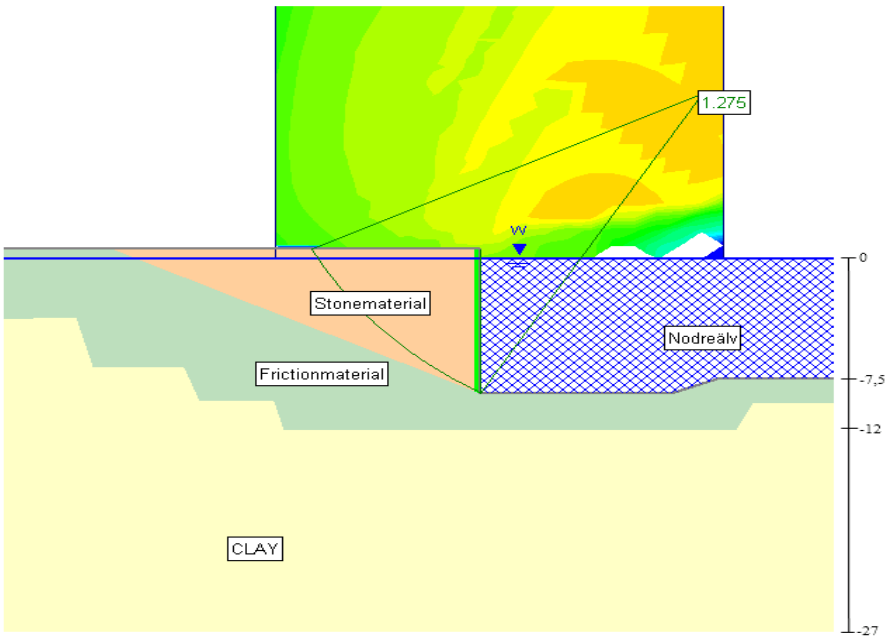

Figure 4.1 Critical slip surface with the normal water level

5. Partial Factors

Stability analysis of the east tower is made according to ultimate limit state method. To satisfy the ultimate limit state, the tower must not collapse when it is subjected to the design peak loads. By applying the partial factor method is created a sufficient safety for the construction by introducing various partial factors.

The design of piles for ultimate limit state condition the general requirement for the application of partial factors is:

$$R \geq S \qquad (5.1)$$

R - Load capacity

S - Load effect

R is the smallest of R_1 or R_2

Where:

R_1 - Constructive load capacity

R_2 - Geotechnical load capacity

According to partial factors method there is an adequate safety if the load capacity is at least as large as or bigger than the load effect.

5.1 Partial Factor Method

In the design according to the partial coefficient method is characteristic values used. For all loads regarding to design are safety built by multiplying the characteristic loads with a partial factor (γ_f). And the design load, with index d, is given by:

$$q_d = \gamma_f \cdot q_k$$

γ_f = 1,0 applying for permanent bounded load (BKR, 2003).

γ_f = 1,3 applying for variable load (BKR, 2003).

For strength of material design is safety built by dividing the characteristic value with a partial factors γ_m and γ_n. The design value on a material property is determined by the formula:

$$f_d = \frac{f_k}{\gamma_m \cdot \gamma_n}$$

Partial factors used in hand calculation and computed into Rymdpålgrupp software is summarized in table below.

Table 5.1 Partial factors

Parameter	*Symbol*	*Value (ultimate limit state)*
Partial factor for soil parameter, tan Φ	$\gamma_{m\Phi}$	*1,2*
Partial factor for soil parameter The other strength parameters	γ_m	*1,6*
Partial factor for permanent load	γ_f	*1,0*
Partial factor for variable load	γ_f	*1,3*
Partial factor for safety class	γ_n	*1,0*
Partial factor for the uncertainty in the calculation	γ_{Rd}	*1,7*

Partial factor for soil parameter (γ_m) vary between 1,6-2,0. If conditions are in all consideration favorable according to table below the lower value should be chosen. If the number of unfavorable factors is large a value in the upper part of the interval should be chosen (Pålgrundläggning, SGI 1993).

Favorable conditions	*Unfavorable conditions*
The material show small scatter	*The material show large scatter*
Laboratory test show a normal scatter	*Laboratory test show a large scatter*
Test results show normal scatter	*Test results show large scatter*
The extent of the investigation is comprehensive	*The extent of investigation is not comprehensive*
Failure will be ductile	*Failure will be brittle*

For each construction will the safety class (SK) be selected as:

SK 1 (low), at risk for minor personal injury, SK 2 (normal), at risk for some personal injury, SK 3 (high), at high risk of personal injury. In the design choose of safety class are considered by partial factor (γ_n).

Where: $\gamma_n = 1{,}0$ Safety Class 1; $\gamma_n = 1{,}1$ Safety Class 2 and $\gamma_n = 1{,}2$ Safety Class 3

Consequence of possible collapse of the Ormo tower may be considered to cause minor injuries.

6. Lateral and Vertical Loads

Since the load duration has greater or lesser impact on strength of construction material, distinguishes between permanent actions (i.e., gravity, soil loading) and variable loads (i.e. wind load) are important (Pålgrundläggning, SGI 1993).

6.1 Wind Load

Wind load on a surface is proportional to the square of wind speed at which an increase in wind speed by 10 % gives a load increase of 20 %. A study has been made by the Swedish Meteorological and Hydrological Institute how the wind has varied in Sweden during the period 1901-2008. In Fig 6.1 shows maximum value of the maximum wind gust for the period 1961-1990. Maximum wind gust is the maximum wind-on-year. The wind is calculated every 30 minutes. According to SMHI scenarios, the extreme winds will increase over the next few years compared to 1961-1990 (Figure 6.2). The Swedish building administration discuss with SMHI to calculate the new characteristic load values for design wind loads (Building and Planning, 2007, Buildings and Climate Change).

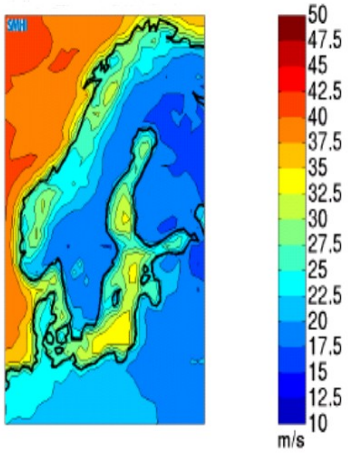

Figure 6.1 Maximum wind gust for the period 1961-1990 (Rossby Centre SMHI)

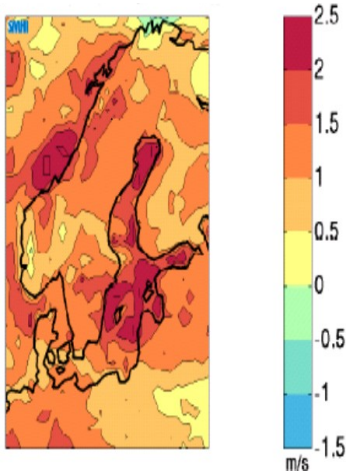

Figure 6.2 Difference of the maximum wind gust 2011-2040 compared with 1961-1990 (Rossby Centre SMHI)

The Ormo's tower fall within the light blue portion of a bar on Figure 6.1 where the maximum wind gust for the period 1961-1990 are up to 25 m/s. This means that the estimated difference on Figure 6.2 is between 1 and 1.5 according to Rossby Centre, SMHI. In other words, an increase of about 5-10 % should be expected during the period 2011-2040 for the east tower.

Wind load is in its nature a dynamic load. This must be considered when determining the load and the design value. For structures with high stiffness and damping the structural vibration characteristics are not taken into account for the determination of wind load.

The change in wind climate has been studied using several different measures, including:

- The highest wind speed
- Average wind speed
- Number of cases of 25 m/s during the years

The reference value of wind velocity (v_{ref}) is 25 m/s for Kungälv municipality close to the tower. This value is shown in Figure 6.3 (Swedish Building Administration, BSV 97, Handbook of wind load).

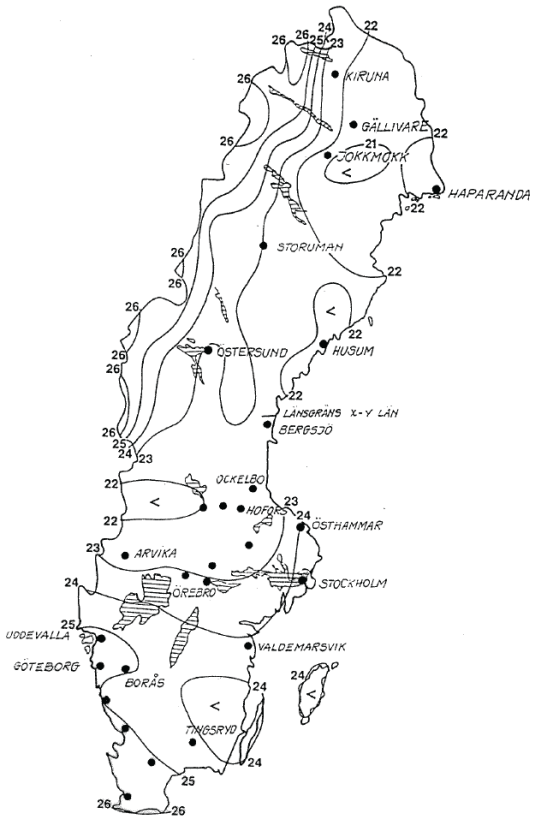

Figure 6.3 Reference wind speed [m/s] in Sweden, (BSV 97, Handbook of wind load)

Reference wind speed is defined by the following three conditions:

- Reference height of 10 m above ground level
- Mean wind speed for 10 minutes
- Terrain type

Probability of being exceeded is 0.02 per year, which means that average return is once in 50 years, i.e., v_{ref} is a characteristic value.

To be able to study the wind climate over a longer period of time a well-established method is to calculate the so-called geostrophic wind from air pressure observations from three locations which form a triangle over the study area. There are 11 investigation triangles over Sweden shown in Figure 6.4

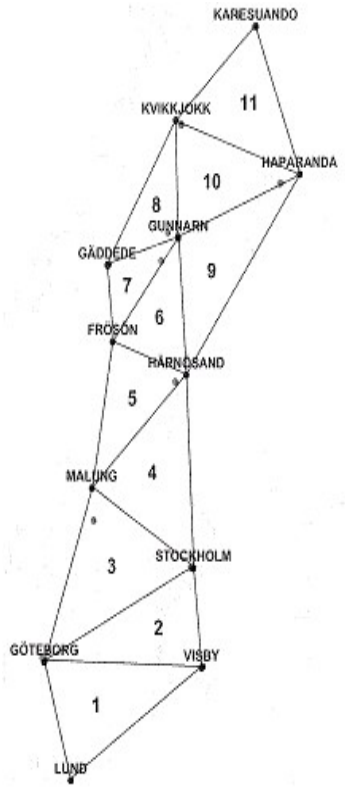

Figure 6.4 Stations and triangles used in analysis

Table 6.1 summarizes developments in geostrophic wind from 1901 and 1951. The triangle 1 and 2 were analyzed for the period 1901 to 2008 while other triangles only for the period 1951 - 2008.

Table 6.1 Linear change in geostrophic wind statistics for Sweden (increases in wind speed are marked in blue, SHHI Nr 138/ 2009)

Period	Triangel	Max vind-hastighet
1901 – 2008	1	-3 %
	2	-19 %
1951 – 2008	1	7 %
	2	12 %
	3	-7 %
	4	-2 %
	5	14 %
	6	9 %
	7	-1 %
	8	-2 %
	9	5 %
	10	-1 %
	11	-1 %
	Medelvärde	3 %

The highest wind speed has increased for triangle 2 but decreased for triangle 3. Data from both triangles is significant for Ormo plant located in the left corner of the triangles. Taking data for triangle 2 with 12 % increase only of interest for tower's stability we will get:

$$v = 25 \cdot 0{,}12 = 28 \text{ m/s}$$

The main wind direction according to SMHI report 138/2009 of the triangle 2 is shown in Figure 6.5. Prevailing geostrophic wind direction is straight west (about 270°) around 1910. Then wind direction turned some south until 1960 – 1970. After 1970 the wind direction turned slowly back towards the straight west. Frequency of wind speed divided in different wind directions (wind roses) and for case when the geostrophic wind speed was at least 25 m/s for period 1991-2008 over triangle 2, Göteborg – Stockholm – Visby is presented in Appendix VI. We see that wind from west and northwest for both cases becomes more common in the last 18 years.

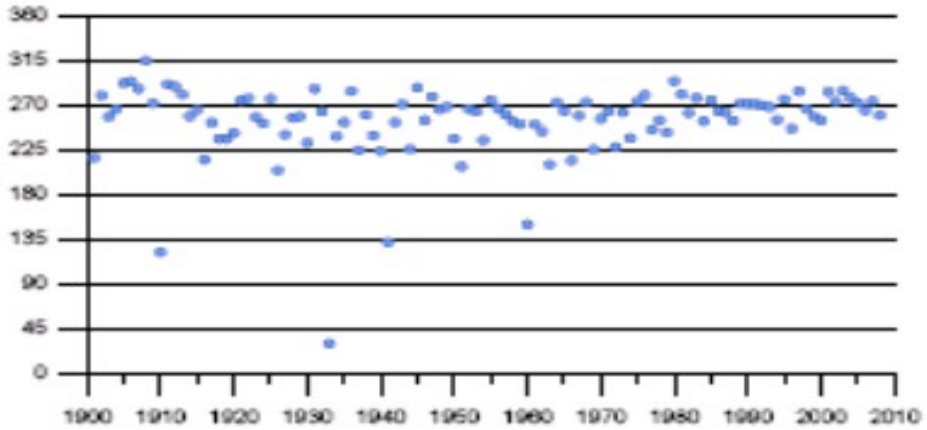

Figure 6.5 Prevailing wind directions 1990-2010 for triangle 2, SMHI Nr138/2009

January 8 and 9, 2005 the gusts of 30,9 m/s (maximum value that lasts a few seconds) was recorded in Göteborg Weather Station (SMHI Nr 2005-42). Wind direction as shown in the figure 6.6 was typical west, south-west and south, i.e between 180 and 270 degrees.

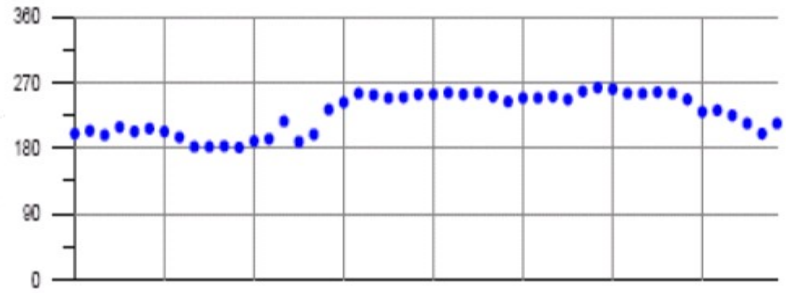

Figure 6.6 Wind direction 8-9 January 2005, Göteborg, SMHI Nr 2005-42

Momentary speed of 30,9 m/s has a return period of 100 years. This value is reached or exceeded on average once in 100 years, which means that the probability is 1 in 100 for each year. Since the tower is exposed to the risk for several years, the cumulative risk will be much greater. For a structure whose lifetime is estimated to be 100 years, the cumulative risk is 63 % that 100-year value will be exceeded at any time during the 100 years, see table 6.2 (Magnus Asp - Klimatdata SMHI).

Table 6.2 Cumulative risk for different return periods (Klimatdata SMHI)

Return period	*Probability over 10 years*	*Probability over 20 years*	*Probability over 50 years*	*Probability over 100 years*
10 years	*65 %*	*88 %*	*99%*	*100 %*
20 years	*40 %*	*64 %*	*92 %*	*99 %*
50 years	*18 %*	*33 %*	*64 %*	*87 %*
100 years	*10 %*	*18 %*	*39 %*	*63 %*

Estimates of wind loads were made according to Swedish Building Administration and Eurocode1.

6.1.1 Wind Load in accordance to BSV 97

Wind velocity is dependent on the terrain characteristics. According to BSV 97 there are four terrain categories:

I Open terrain with few or no obstacles (such as coasts and beaches in open water, distinctly flat land)

II Open ground with small obstacles (i.e. spreading trees and occasional groups of buildings)

III Terrain with scattered large obstacles (i.e, suburban housing, less urban areas)

IV Urban area where at least 15% is built and the average buildings height is > 15 m

As explained above the Ormo Screen Plant suppose to belongs the category (II), with corresponding roughness length Zo=0,05 m and terrain factor β=0,19.
In order to calculate the total wind load the tower is divided into 10 narrow strips or elements according to Figure 3.1 and 6.7. Each element is 2 m thick except the first and last one. The first one has height of 4 and the last one 6 m which is the roof of the building. The velocity pressures are uniform for each horizontal part. As seen on the same figure the minimum height below which the exposure factor (Cexp) is constant is given from the table 2:22a (Boverkets handbok om snö- och vindlast BSV 97, Zmin=4 m for category II).

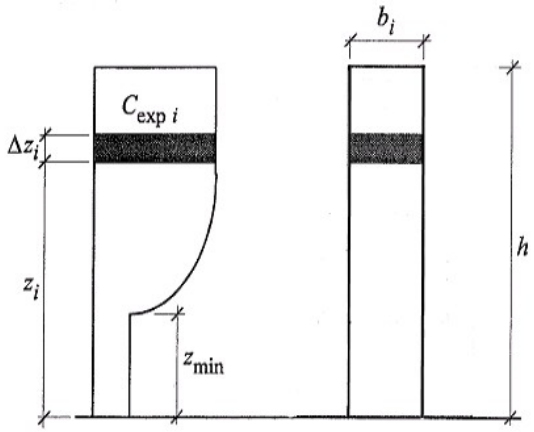

Figure 6.7 Division of the tower into the narrow strip

Where:

Δz_i=element's hight

bi=5,66 (element's width)

h=24 m (tower's height above the water level)

Using the v_{ref} =25m/s from Figure 6.3 reference velocity pressure, q_{ref} are counted from equation (6.1).

$$q_{ref} = \frac{1}{2}\rho v_{ref}^2 = 0{,}39\,kN/m^2 \quad (6.1)$$

ρ=1,25 kg/m³ (air density)

To be able to calculate characteristic wind load *Wk* the characteristic velocity pressure q_k for each element are determined from equation (6.2).

$$q_k = C_{dyn} \cdot C_{exp} \cdot q_{ref} \quad (6.2)$$

Where:

The gust factor C_{dyn} are calculated as:

$$C_{dyn} = 1 + \frac{6}{\ln\left(\frac{h}{Z_0}\right)} = 1{,}97 \qquad (h \geq z \text{ min})$$

And the exposure factor *Cexp(z)* are obtained from equation (6.3).

$$C_{\exp}(z) = \left[\beta \cdot \ln\left(\frac{z}{Zo}\right)\right]^2 \quad (6.3)$$

The characteristic wind load *Wk* is then determined from equation 6.4 (BSV 97).

$$Wk = \mu \cdot q_k \cdot A \quad (6.4)$$

Form factor (μ) for windward-, leeward side and roof will be chosen from Figure 6.8 and 6.9. In order to receive the requested form factor (μ) the level of elements height is divided by element's width (*z/b)*.

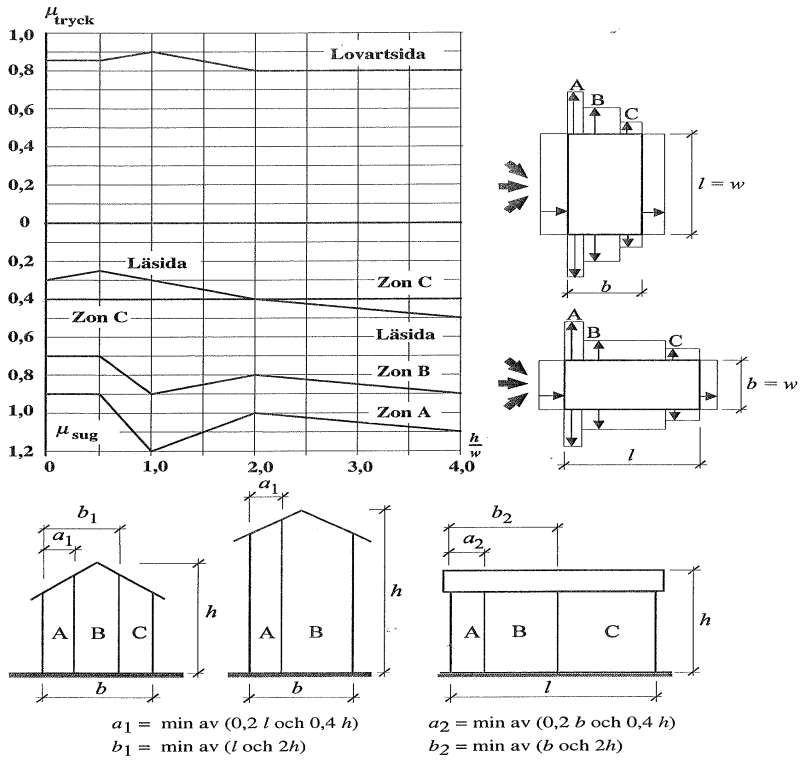

Figur 6.8 Form factors for walls

The form factor of the roof surface A, B, C, D, E depend of *x* and *y*. These are defined as: *x=l* and *y=b* i.e *x= y=5,66*.

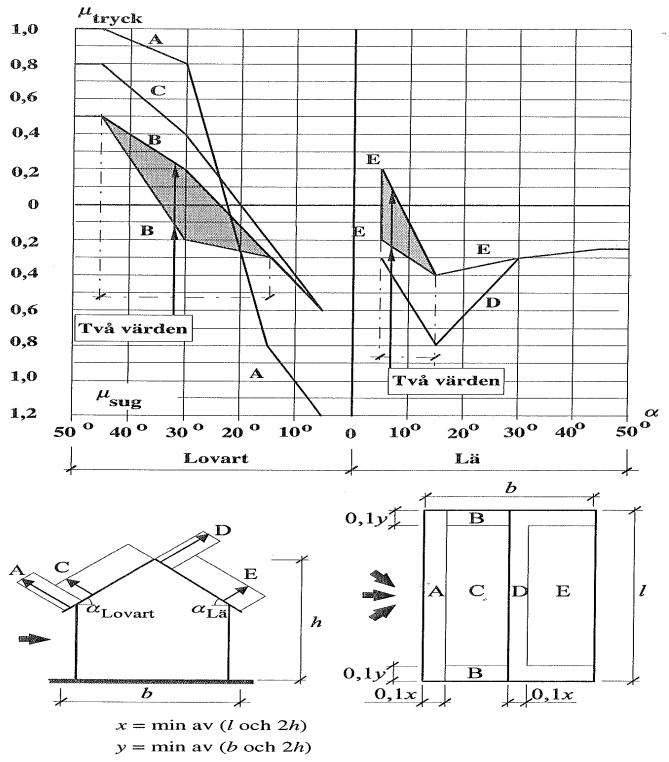

Figure 6.9a Form factors for roof (α>5°)

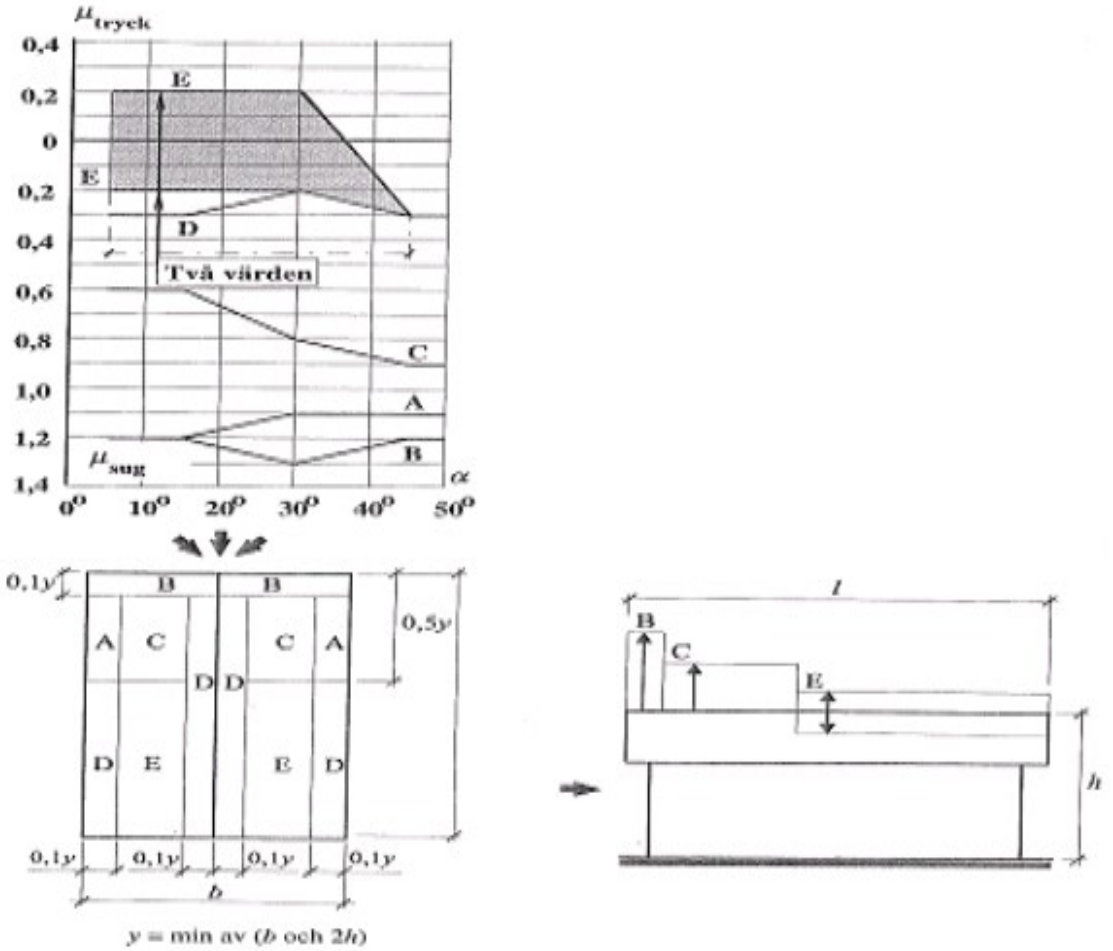

Figure 6.9b Form factors for roof (α>5°)

The area of surfaces for wall (A) and roof (A_A, A_B, A_C, A_D, A_E) of the tower are calculated in Table 6.3.

Summary of all form factors with the area of each elements and the result of wind loads, together with the corresponding moments for cases with wind speed of 25 m/s are presented in the table below. Wind loads are calculated in the east/west-EW, south/north-SN or north/south-NS direction.

Table 6.3a Summary of form factors, characteristic velocity pressures, exposure factors and areas for each element

z (m)	*C exp*	*q_k(kN/m^2)*	*A (m^2)*	*z/b*	*μ (ww)*	*μ (lw)*
4	*0,69*	*0,53*	*22,64*	*0,71*	*0,87*	*0,28*
6	*0,83*	*0,64*	*11,32*	*1,06*	*0,90*	*0,30*
8	*0,93*	*0,72*	*11,32*	*1,41*	*0,85*	*0,33*
10	*1,01*	*0,78*	*11,32*	*1,77*	*0,82*	*0,38*
12	*1,08*	*0,84*	*11,32*	*2,12*	*0,80*	*0,40*
14	*1,15*	*0,88*	*11,32*	*2,47*	*0,80*	*0,41*
16	*1,20*	*0,93*	*11,32*	*2,83*	*0,80*	*0,43*
18	*1,25*	*0,96*	*11,32*	*3,18*	*0,80*	*0,45*
20	*1,30*	*1,00*	*11,32*	*3,53*	*0,80*	*0,46*
24	*1,37*	*1,05*	*11,32*	*4,24*	*0,80*	*0,50*
Roof EW	*AB(m^2)*	*3,2*	*AC(m^2)*	*10,25*	*AE(m^2)*	*12.8*
Roof SW	*AA(m^2)*	*3,2*	*AC(m^2)*	*12*	*AD(m^2)*	*5,9*
μ (45°) EW	*μ (B)*	*μ (C)*	*μ (E)*			
	1,2	*0,9*	*0,3*			
μ (45°) SW	*μ (A)*	*μ (B)*	*μ (C)*	*μ (D)*	*μ (E)*	
	1	*0,5*	*0,8*	*0,25*	*0,25*	

Table 6.3b Results of the wind loads and moment for v_{ref}=25m/s - EW and SN

z (m)	*Pilecap (m)*	*W(kN) EW*	*Wd-EW*	*Mk(kNm)-EW*	*Md-EW*	*W(kN)-SN*	*Wd-SN*	*Mk(kNm)-SN*	*Md-SN*
4	*12,4*	*14,74*	*19*	*183*	*238*	*14,74*	*19*	*183*	*238*
6	*14,4*	*9,18*	*12*	*132*	*172*	*9,18*	*12*	*132*	*172*
8	*16,4*	*10,14*	*13*	*166*	*216*	*10,14*	*13*	*166*	*216*
10	*18,4*	*11,24*	*15*	*207*	*269*	*11,24*	*15*	*207*	*269*
12	*20,4*	*12,03*	*16*	*245*	*319*	*12,03*	*16*	*245*	*319*
14	*22,4*	*12,82*	*17*	*287*	*373*	*12,82*	*17*	*287*	*373*
16	*24,4*	*13,66*	*18*	*333*	*433*	*13,66*	*18*	*333*	*433*
18	*26,4*	*14,45*	*19*	*381*	*496*	*14,45*	*19*	*381*	*496*
20	*28,4*	*15,09*	*20*	*429*	*557*	*15,09*	*20*	*429*	*557*
24	*32,4*	*33,51*	*44*	*1086*	*1451*	*18,31*	*24*	*593*	*771*
	Σ	*146,86*	*193*	*3449*	*4524*	*132*	*173*	*2956*	*3844*

The total characteristic wind load on a tower is the sum of wind load for each element

$$Wk(EW) = 147\ kN$$

$$Wk(SN) = 132\ kN$$

The design value of the wind force are calculated by multiplying the total characteristic wind load with partial factor for variable load (γ_f).

$$Wd = \gamma_f \cdot Wk$$

The moment is obtained by multiplying wind force for each element by elevation above the pile cap.

The results of wind loads and moment for cases with wind speed of 28 m/s and 30,9 m/s are presented in the tables below. The reader can easily realize that the increase of wind loads is approximately 20 % between the calculated reference speeds.

Table 6.4 Results of the wind loads and moment for v=28m/s -EW and SN

W(kN)-EW	*Wd-EW*	*Mk(kNm)-EW*	*Md-EW*	*W(kN)-SN*	*Wd-SN*	*Mk(kNm)-SN*	*Md-SN*
176	*229*	*4159*	*5407*	*157*	*204*	*3541*	*4603*

Table 6.5 Results of the wind loads and moment for v =30,9m/s

W(kN)-EW	*Wd-EW*	*Mk(kNm)-EW*	*Md-EW*	*W(kN)-SN*	*Wd-SN*	*Mk(kNm)-SN*	*Md-SN*
215	*279*	*4963*	*6452*	*191*	*249*	*4257*	*5534*

Wind load can be applied to all sides of construction. Stability calculations have been made by studying the wind directions that interact with other horizontal loads on the tower. The western wind has the opposite direction to the horizontal load from the fill and was not interesting in the calculations. The most interesting wind on the tower's stability is the easterly wind that interacts with the load from the fill. Even comparison with the wind load caused by north wind, which has the same direction as the pressure from the stream of water and south wind was calculated.

6.1.2 Wind Load in accordance to Eurocode 1

In Eurocode 1, has introduced new designation for the same notions as compared with BSV 97. To see the difference in the designations, the names were collected and equal sign stands between the same designations as follows:

Eurocode 1	BSV 97
v_b *basic wind velocity*	v_{ref} *reference value for wind speed*
q_b *basic velocity pressure*	q_{ref} *reference velocity pressure*
q_p *peak velocity pressure*	q_k *characteristic velocity pressure*
$c_e(z)$ *exposure factor*	$C_{exp}(z)$ *exposure factor*
Cp pressure coefficient	μ *Form factor*

As explained in the previous chapter the wind loads calculated by Eurocode 1 are determined for the basic wind velocity (q_b) of 25 but also 28 and 30,9 m/s. The wind pressure for each element acting on the external surfaces (*We*), are obtained from expression (6.4).

$$Wk=q_p(Z_e)\cdot Cpe\cdot A \qquad (6.4)$$

Where:

$$q_p(Z_e)=Ce(z)\cdot q_b$$

$$q_b = \frac{1}{2}\rho v_b^2$$

The exposure factor *Ce(z)* is illustrated in Figure 6.10 as a function of height above terrain and a function of terrain category.

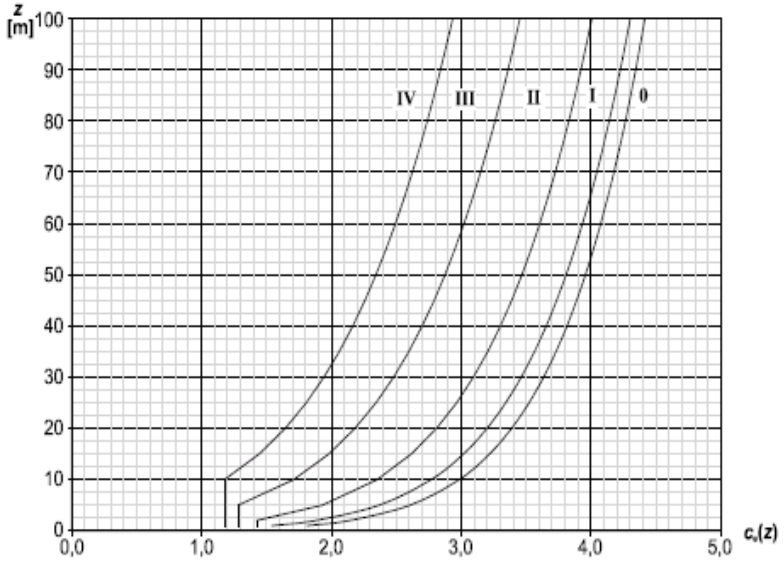

Figure 6.10 Illustrations of the exposure factor Ce(z)-(EN 1991-1-4)

According to Eurocode there are 5 terrain categories. *Zo* and *Zmin* depend on the terrain category. All the categories are summarized in Table 6.6. The Ormo Screen Plant belongs to the category (II).

Table 6.6 Terrain category (EN 1991-1-4)

Terrain category		z_0 m	z_{min} m
0	Sea or coastal area exposed to the open sea	0,003	1
I	Lakes or flat and horizontal area with negligible vegetation and without obstacles	0,01	1
II	Area with low vegetation such as grass and isolated obstacles (trees, buildings) with separations of at least 20 obstacle heights	0,05	2
III	Area with regular cover of vegetation or buildings or with isolated obstacles with separations of maximum 20 obstacle heights (such as villages, suburban terrain, permanent forest)	0,3	5
IV	Area in which at least 15 % of the surface is covered with buildings and their average height exceeds 15 m	1,0	10

In accordance to figure 6.11 for a building whose height (*h*) is greater than 2b the tower are divided into 8 parts. Each part is 5,66 breadth and 2 m thick except the first and last one which has height of 6 m. The velocity pressures are uniform for each horizontal part.

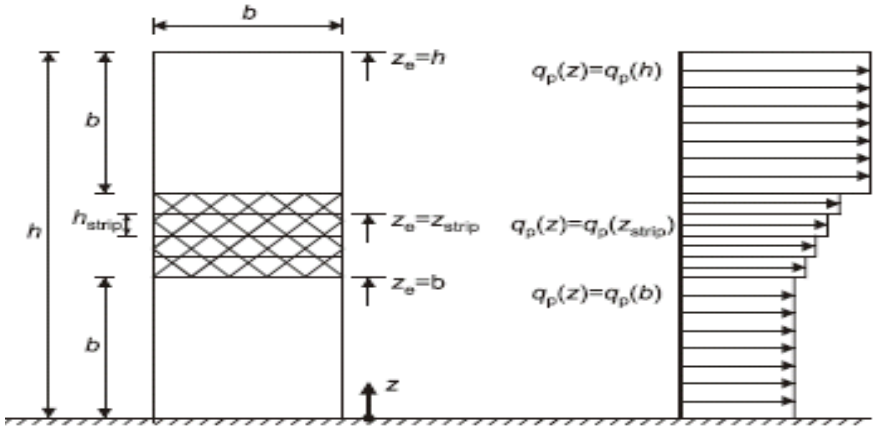

Figure 6.11 Referenceheight, Ze and velocity pressure profile (EN 1991-1-4)

The external pressure coefficients for tower depend on the ratio (*h/d*). Values for walls (zones A,B,D,E) and duopitch roof of 45° (F,G,H,J,I) are given in table 6.7.

Table 6.7 External pressure coefficient Cpe for walls and roof α= 45°(EN 1991-1-4)

Zone	*A*	*B*	*D*	*E*	
h/d	*Cpe*	*Cpe*	*Cpe*	*Cpe*	
5	*-1,2*	*-0,8*	*0,8*	*-0,7*	
1	*-1,2*	*-0,8*	*0.8*	*-0,5*	
Zone	*F*	*G*	*H*	*I*	*J*
θ= 0°	*0,7*	*0,7*	*0,6*	*0*	*0*
θ= 90°	*-1,1*	*-1,4*	*-0,9*	*-0,5*	

For intermediate values of h/d linear interpolation are used. Key zones (D, E) for walls and (F, G, H, I, J) for roof are defined in figure 6.12 and 6.13.

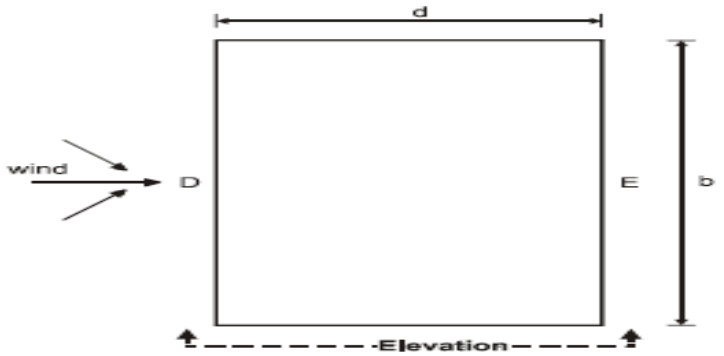

Figure 6.12 Key zones for vertical walls (EN 1991-1-4)

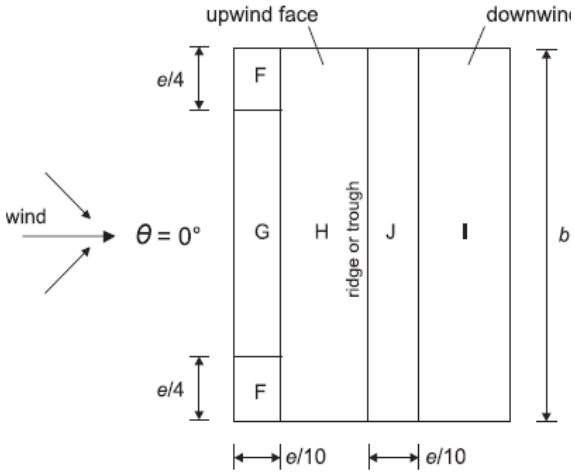

Figure 6.13a Key for duopitch roofs for θ= 0°, e=b (EN 1991-1-4)

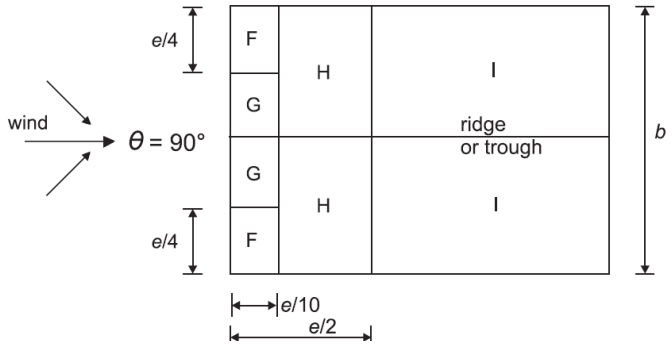

Figure 6.13b Key for duopitch roofs for θ= 90°, e=b (EN 1991-1-4)

Summation of all pressure coefficients, exposure factor and peak velocity pressure together with the calculated wind forces and their locations above the pile cap are shown in table 6.8. All wind loads are horizontal and are calculated in z and y-direction.

Table 6.8a Summery of all pressure coefficient, exposure factor, peak velocity pressure and area of roof zones for v_b =25m/s

z (m)	*Ce(z)*	*qp(Ze) (kN/m²)*	*Cpe(ww)*	*Cpe(lw)*		
6	*2*	*0,78*	*0,8*	*0,5*		
8	*2,22*	*0,87*	*0,8*	*0,52*		
10	*2,35*	*0,92*	*0,8*	*0,53*		
12	*2,47*	*0,96*	*0,8*	*0,55*		
14	*2,58*	*1,01*	*0,8*	*0,57*		
16	*2,67*	*1,04*	*0,8*	*0,58*		
18	*2,77*	*1,08*	*0,8*	*0,6*		
24	*2,95*	*1,15*	*0,8*	*0,65*		
Roof EW	*AG(m²)*	*1,6*	*AH(m²)*	*12,8*	*AI(m²)*	*16*
Roof SN	*AG(m²)*	*2,7*	*AH(m²)*	*14,4*	*AI(m²)*	*14,4*
			Aj(m²)	*3,6*		

Table 6.8b -Results of the wind loads and moment for v_b =25m/s

z(m)	*Pilecap-(m)*	*W(kN) EW*	*Wd-EW*	*Mk(kNm)-EW*	*Md-EW*	*W(kN) SN*	*Wd-SN*	*Mk(kNm)-SN*	*Md-SN*
6	*14,4*	*34*	*45*	*497*	*646*	*34*	*45*	*497*	*646*
8	*16,4*	*13*	*17*	*213*	*276*	*13*	*17*	*213*	*276*
10	*18,4*	*14*	*18*	*254*	*331*	*14*	*18*	*254*	*331*
12	*20,4*	*15*	*19*	*301*	*391*	*15*	*19*	*301*	*391*
14	*22,4*	*16*	*20*	*350*	*455*	*16*	*20*	*350*	*455*
16	*24,4*	*16*	*21*	*398*	*517*	*16*	*21*	*398*	*517*
18	*26,4*	*17*	*22*	*453*	*589*	*17*	*22*	*453*	*589*
24	*32,4*	*57*	*74*	*1848*	*2402*	*12*	*16*	*393*	*511*
	Σ	*182*	*237*	*4313*	*5606*	*137*	*178*	*2858*	*3715*

The results of wind loads and moment for cases with wind speed 28 m/s and 30,9 m/s are presented in the tables below.

Table 6.9 Results of the wind loads and moment for v_b =28m/s

W(kN) EW	*Wd-EW*	*Mk(kNm)-EW*	*Md-EW*	*W(kN) SN*	*Wd-SN*	*Mk(kNm)-SN*	*Md-SN*
228	*297*	*5410*	*7033*	*172*	*224*	*3585*	*4660*

Table 6.10 Results of the wind loads and moment for v_b =30,9m/s

W(kN) EW	*Wd-EW*	*Mk(kNm)-EW*	*Md-EW*	*W(kN)-SN*	*Wd-SN*	*Mk(kNm)-SN*	*Md-SN*
278	*362*	*6588*	*8565*	*210*	*273*	*4366*	*5676*

6.2 Lateral Earth Pressure

The load from the embankment is pressing the eastern side of the tower from +0.86 to -7,5 m, as shown Figure 2.1 where the towers foundation lies.

The lateral earth pressure (Pa) is the active earth pressure i.e the tower is moving away from the embankment. It is given by the classical earth pressure theory (equation 6.5), i.e the effective vertical stress at the foundation level ($\sigma_0^{'}$) multiplied by lateral earth pressure coefficient K_A (Sällförs, 2001).

$$Pa = \sigma_0^{'} \cdot K_A \qquad (6.5)$$

Effective vertical stress is obtained from (equation 6.6).

$$\sigma_0^{'} = \Sigma \gamma_i z_i \qquad (6.6)$$

z_i - Layer thickness (m).

γ_i - Unit weight of material (kN/m^3)

From Table 2.1 the unit weight of gravel are the same as of stone, γ = 18 kN/m^3 and effective unit weight is γ' = 11 kN/m^3.

By using equation (6.6) effective vertical stress are estimated:

$$\sigma_0^{'} = 7{,}5m \cdot 11kN/m^3 + 0{,}86m \cdot 18kN/m^3 = 98kPa$$

The design value for the earth's internal friction angle (ϕ_d) is obtained from equation (6.7).

$$\phi_d = \tan^{-1}\left(\frac{\tan\phi}{\gamma_{m\phi}\cdot\gamma_n}\right)=30° \qquad (6.7)$$

$\gamma_{m\phi}$ = 1,2 (Pile foundation SGI, 1993, table 6.15:5).

γ_n = 1,0

ϕ_k = 35°, the characteristic value of friction angle taken from table (2.1)

Table 6.11 Examples of typical values for the internal friction angle ϕ_k, (Handboken bygg, Geoteknik,1984)

Stratification	*Sand*	*Gravel*	*Sandy moraine*	*Gravelly moraine*	*Macadam*	*Stone*
Loose	*28°*	*30°*	*35°*	*38°*	*30°*	*40°*
Solid	*35°*	*37°*	*42°*	*45°*	*38°*	*45°*

The active earth pressure coefficient K_A is computed by equation (6.8).

$$K_A = \tan^2(45 - \phi_d/2) = \tan(28,6) = 0,57^2 = 0,3 \qquad (6.8)$$

The horizontal earth pressure (*Pa*) increases linearly with depth and will be the half as large. By using the values of total vertical stress and lateral earth pressure coefficient the horizontal earth pressure (*Pa*) are calculated:

$$Pa = 98 \cdot 0,3 / 2 = 14,7\ kN/m^2$$

Because the earth pressure is zero at the edges of the embankment approximately only 2/3 of the total area (see Figure 6.14) that contribute to the horizontal force on the east side of the tower. The cross-sectional area of the embankment is shown in Figure 6.14.

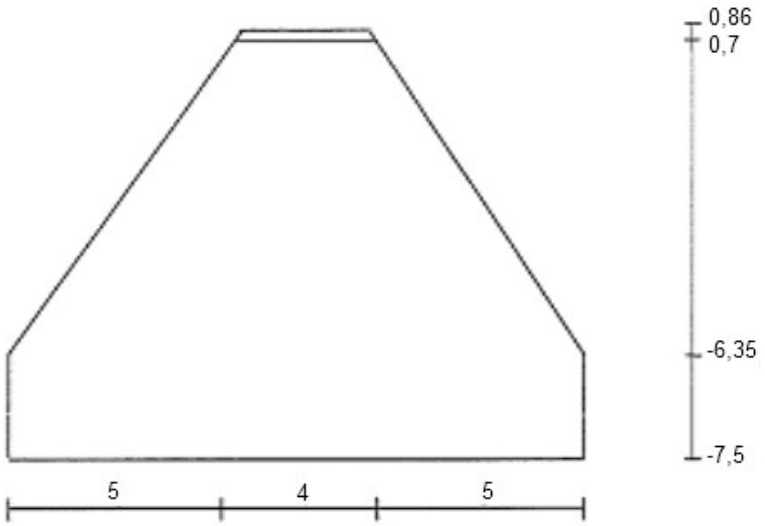

Figure 6.14 Cross-section area of the embankment (the vertical scale shows the altitude above and below water level and the horizontal scale shows dimensions in meters)

The effective area is thus equal to:

$$A = 8{,}36\text{m} \cdot 4\text{m} + 1{,}15\text{m} \cdot 5\text{m} + 7{,}21 \cdot 5 / 2 = 57\ m^2$$

The design value of the horizontal force from embankment is calculated by multiplying the horizontal earth pressure (*Pa*) with the effective area and the partial factor for permanent load (γ_f).

$$H_{embankment} = 1{,}0 \cdot 14{,}7\ kN/m^2 \cdot 57\ m^2 = 840{,}69\ kN$$

The horizontal force are located 2,79 m above the base of the embankment.

$$(7{,}5 + 0{,}86) \cdot 1/3 = 2{,}79\ m$$

Bending moment on the pile cap is calculated as vector moment *Mx, My, Mz*. The moment is positive for clockwise rotation, round current positive axis directions. Moment of the horizontal force $H_{embankment}$ with regard to y-axis is derived from the expression:

$$My = 840{,}69 \cdot 2{,}79 = 2343\ kNm$$

6.3 Water Pressure

Photo 4 The Ormo Plant with the screen wall

The water pressure on the tower is calculated when the screen is closed as shown on the photo above. It should be noted from the same photo that the screen is open on the left side closest to the east tower.

The difference between the upstream and downstream water level when the screen are closed can maximum be 20 cm (Forsberg et al, 2002).

The total water pressure along the screen which is connected to the east tower can be calculated as:

$$Pw = \frac{\Delta h \cdot \gamma_w (h_2 + h_1)}{2} = \frac{0{,}2 \cdot 10 \cdot (7{,}7 + 7{,}5)}{2} = 15{,}2 kN/m$$

Where: $\Delta h = h_2 - h_1 = 0{,}2\ m$

$h_2 = 7{,}7$ (water level from the upstream side of the screen)

$h_1 = 7{,}5$ (water level from the downstream side)

Δh - water level difference

$\gamma_w = 10\ kN/m^3$, unit weight of water

The horizontal force from the water load is given as the total water pressure multiplied by the length of the screen wall (L_{screen}). Because the half of this force is transferred to the east tower the final value will be:

$$H_{water} = 15{,}2\ kN/m \cdot 37m/2 = 281\ kN$$

$L_{screen} = 37\ m$

And finally to get the design value the above value will be multiplied by partial factor of safety for variable load (γ_f).

$$H_{water} = 281\ kN \cdot 1{,}3 = 365\ kN$$

The horizontal force H_{water} acting on the east tower in positive (y) direction and has its attack point 3,75 m above the pile cap. Its moment with regard to x- and z-axis is derived from the expression:

$$Mx=-365\cdot4,5=-1642,5\ kNm$$

$$Mz=-365\cdot3,75=-1369\ kNm$$

6.4 The Tower's Weight

The vertical force is composed due to self weight of east tower. The tower consists of material with varying unit weight as concrete, timber and steel. Material inventory of all construction part with names of material, number and dimensions in meter are shown in Table 6.12 below and in Appendix III. The material includes steel for the main frame, wood for the wall and reinforced concrete for caisson and plate.

The weight of the mechanical system, which is responsible for the lowering and lifting up of the screen, is considered to be equal to sum weight of the counter tank 100 kN and tank filled with water 400 kN.

Table 6.12-Construction elements of East Tower

Part I - Concrete

Element	*B-Width*	*H-Height*	*L-length*	*Number*	*Sum*	*Density*	*Units*
Heel	*3*	*1,3*	*9*		*35,1*		m^3
Plate	*9*	*1,2*	*15*		*162*		m^3
Caisson	*0,3*	*10,1*	*14*	*2*	*84,84*		m^3
	0,3	*10,1*	*6*	*2*	*36,36*		m^3
	0,2	*10,1*	*6*	*2*	*24,24*		m^3
					342,54	*24*	kN/m^3
				Σ	*8 220,96*		*kN*

Part II Timber

Wood	*Dimensions*	*Sides*	*L*	*Number*	*Sum*	*Density*	*Units*
Beam	*0,075x0,1*	*4*	*6*	*15*	*2,7*		*m^3*
A-A; C-C						*6*	*kN/m^3*
					16,2		*kN*
	0,075x0,1	*4*	*19*	*11*	*6,27*		
					37,62		
Roof	*0,075x0,1*	*2*	*3,1*	*6*	*0,28*	*6*	
					1,67		
B-B; D-D	*0,075x0,1*	*2*	*3,1*		*0,047*	*6*	
					0,28		*kN*
	0,075x0,1	*2*	*2,48*		*0,04*		
					0,22		*kN*
	0,075x0,1	*4*	*1,86*		*0,056*		
					0,33		*kN*
	0,075x0,1	*4*	*1,24*		*0,04*		
					0,22		*kN*
	0,075x0,1	*4*	*0,62*		*0,02*		
					0,11		*kN*
Roof (H-beam)	*0,075x0,1*	*2*	*4*		*0,06*		
					0,36		*kN*
	0,075x0,1	*2*	*2*		*0,03*		
					0,18		*kN*
	0,075x0,1		*1*		*0,01*		
					0,04		*kN*
Paneling	*19x6*	*4*	*0,025*		*11,4*		
Double side x2						*6*	*kNm^3*
					136,8		*kN*
Roof 45° paneling	*6x3,1*	*4*	*0,025*		*1,86*	*6*	
Double side x2					*22,32*		*kN*
				Σ	*216,38*		*kN*

Part III -Steel

Frame-Steel	*Number of sides*	*L-length*	*Number*	*Sum*	*Density*	*Units*
		19	*4*	*76*		*m*
	2	*6*	*6*	*72*		*m*
	2	*6,7*	*6*	*80,4*		*m*
	2	*6*	*6*	*72*		*m*
	2	*6,7*	*4*	*53,6*		*m*
	2	*4,1*	*4*	*32,8*		*m*
	2	*3,5*	*4*	*28*		*m*
				414,8	*20*	*kg/m*
			Σ	*82,96*		*kN*

By summing all parts the total weight of The East Ormo tower is:

$$8\ 220{,}96+216{,}38+82{,}96+400+100 = 9020\ kN$$

The design value of the vertical force due to self weight (V) is calculated by multiplying the value of total weight with partial factor for permanent load (γ_f).

$$V = 9020 \cdot \gamma_f = 9020\ kN$$

The vertical force (V) acting on the east tower in x-direction.

7. Global Structural Capacity

One feature of piles is that they can be subjected to both tensile and compressive forces as shown in Figure 7.1. The loads are transferred to the surrounding soil through the tip of piles, mantle, or a combination thereof. If the pile is beaten to a solid layer it has a certain mantle capacity even if the tip bearing capacity is dominant (Pålgrundläggning, SGI 1993). As it has been mentioned in the Chapter 3, piles are proposed to reach the firm bottom all the way to bedrock as shown on Figure 2.1.

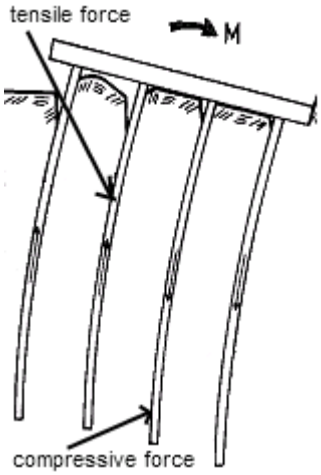

Figure 7.1 Piles exposed to Bending moment, Compressive and Tensile Force (Fleming, 1985, Pålgrundläggning, SGI 1993)

Calculation is performed using software called Rymdpålgrupp version 1.20.20. The program was created by the Software Engineering Company. It calculates statically determined and undetermined pile groups with or without reference to the earth's lateral resistance. Results are presented in form of: cross-sectional forces (*Nx, Vy, Vz, Mx, My, Mz*), displacements and rotations of pile cap. The normal forces are positive in compression load. The pile cap are described below as the counterclockwise corner coordinates in *yz* plane from the lower left (1) to the upper left edge (4) and shown in Figure 7.2

Nr	*y(m)*	*z(m)*
1	7,5	-4,5
2	-7,5	-4,5
3	-7,5	4,5
4	7,5	4,5

The orientation of each pile at the pile cap is given by x, y and z -coordinates. Piles are numbered 1-66, where the piles from 55-66 are with 14° inclination, as calculated in section 3.3.1.

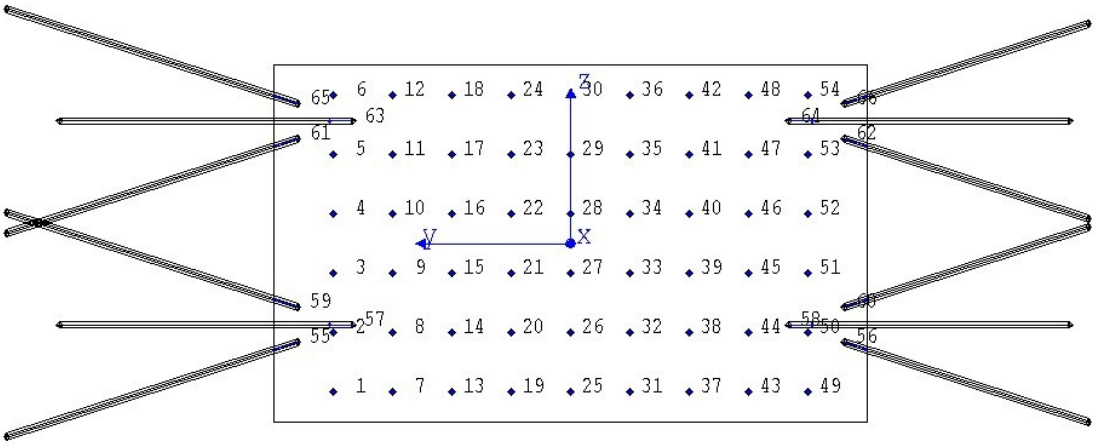

Figure 7.2 The Pile Cap with the x-axis perpendicular to the yz-plane and pile numbers

The piles length to the firm bottom varies between 20 and 24 m as it was pointed out in Chapter 2. All piles have circular cross section with coordinates x = 0:00 and x axis positive downwards.

The pile area will be: $$A = \frac{\pi \cdot d_p^2}{4} = 0{,}025 m^2$$

The following constants of pile are used in the calculation of structural capacity:

a) The moment of inertia of the pile for double symmetric cross section is calculated according to equation 7.1.

$$W = \frac{\pi \cdot d_p^3}{32} = 5{,}7 \cdot 10^{-4} m^3 \qquad (7.1)$$

b) Torsional factor for the pile of circular cross section (Kv) are obtained from (7.2).

$$Kv = \frac{\pi \cdot d_p^4}{32} = 0{,}1 \cdot 10^{-3} m^4 \qquad (7.2)$$

c) The subgrade reaction coefficient (*kd*) is constant with depth and gives as a product of foundation modulus (*bm*) and pile diameter.

$$kd = bm \cdot d_p = 21\ MN/m^3 \cdot 0{,}18\ m = 3{,}75\ MPa$$

$bm = 21\ MN/m^3$, foundation modulus of clay (Handboken bygg, Geoteknik, 1984)

Foundation modulus varies between 20-30 MN/m^3, for softer clays the lower value are selected.

d) Modulus of elasticity for wooden pile E =$10 \cdot 10^6$ kPa (Pile Foundation, SGI, 1993, Table 5.22:1).

e) The shear modulus is calculated from equation (7.3).

$$G = \frac{E}{2 \cdot (1 + \upsilon)} = 4GPa \qquad (7.3)$$

υ = 0,25 Poisson's ratio

Piles are assumed to be pin-jointed at both head and foot as shown in Figure 7.3

Figure 7.3 Piles interconnection

7.1 Load Effect

Load effect is the effect on the pile of all loads. Full impact that different combination of loads has on the pile and all its parts and sections. The load effect of the installed pile in this report refers to the forces, moments, and deformations (translation and the rotations).

All loads are considered as horizontal and vertical point loads with the same load combination (*lk*). Loads are assumed to always act in the global coordinate system directions. Horizontal point loads is described by the coordinates (y) start, (z) start, intensity, height over the origin and direction of the load from the positive y axis counterclockwise. Vertical point load is described by the coordinates (y) start, (z) start and intensity (Software Engineering, Rymdpålgrupp manual).

7.2 Cross-sectional forces

When a pile is loaded by both axial and transversal loading it will generate normal forces, shear forces and moments in the pile element. A pile can take up six load components on pile head, three forces and three moments. These are associated with six kinematic degrees of freedom. It has thus six stiffnesses. Usually the stiffness is neglected about the z axis. In a two-dimensional case, pile head has three degrees of freedom. Often it is neglected even the pile stiffness and load then causes only normal forces in the piles. This involve that the pile becomes a one-dimensional pole element, see Figure 7.4 (Handboken bygg, Geoteknik, 1984).

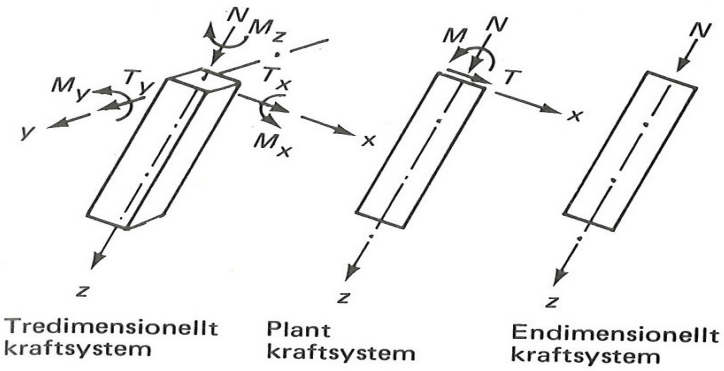

Figure 7.4 Three-, two and one dimension system of cross sectional forces, (Handboken bygg, Geoteknik, 1984)

The structural capacity of the piles is checked by calculating the axial, horizontal and moment load. Thus we get the maximum load on each pile and compare the max value with the capacity of a pile in Chapter 7.4.

7.2.1 The load on the piles caused by east wind

The results are presented in accordance to BSV97 and in accordance to Eurocode 1. The tables have collected information about maximum or minimum normal forces (*Nx*), shear forces (*Vy,Vz*) and bending moment (*Mx,My,Mz*).

Table 7.1 Max / Min cross-sectional forces –BSV97

Forces (kN)	*Nx*	*Vy*	*Vz*	*Mx*	*My*	*Mz*	*Pile*
Max Nx	*183,9*	*-2,8*	*2,1*	*0*	*0,4*	*0,5*	*66*
Min Nx	*93,4*	*-8,5*	*1,7*	*0*	*0,3*	*1,5*	*56*
Max Vy	*97,8*	*5,9*	*0,8*	*0*	*0,2*	*-1,1*	*49*
Min Vy	*132,3*	*-16,5*	*18,2*	*0*	*3,3*	*2,9*	*61*
Max Vz	*176,9*	*-6,1*	*21*	*0*	*3,8*	*1,1*	*65*
Min Vz	*170,9*	*-2,9*	*-1,6*	*0*	*-0,3*	*0,5*	*64*
Max Mx	*151,4*	*-11,5*	*18,3*	*0*	*3,3*	*2,1*	*63*
Min Mx	*170,9*	*-2,9*	*-1,6*	*0*	*-0,3*	*0,5*	*64*
Max My	*176,9*	*-6,1*	*21*	*0*	*3,8*	*1,1*	*65*
Min My	*101,9*	*-8,3*	*-1,6*	*0*	*-0,3*	*1,5*	*58*
Max Mz	*132,3*	*-16,5*	*18,2*	*0*	*3,3*	*2,9*	*61*
Min Mz	*97,8*	*5,9*	*0,8*	*0*	*0,2*	*-1,1*	*49*

Table 7.2 Max / Min cross-sectional forces –Eurocode 1

Forces (kN)	*Nx*	*Vy*	*Vz*	*Mx*	*My*	*Mz*	*Pile*
Max Nx	*192,9*	*-3*	*1,5*	*0*	*0,3*	*0,5*	*66*
Min Nx	*87,2*	*-8,4*	*1,1*	*0*	*0,2*	*1,5*	*56*
Max Vy	*88,6*	*5,9*	*1,5*	*0*	*0,3*	*-1,1*	*49*
Min Vy	*137,7*	*-16,9*	*18,8*	*0*	*3,4*	*3*	*61*
Max Vz	*185,9*	*-6,2*	*21,6*	*0*	*3,9*	*1,1*	*65*
Min Vz	*178*	*-3,2*	*-2,3*	*0*	*-0,4*	*0,6*	*64*
Max Mx	*158,5*	*-11,8*	*18,9*	*0*	*3,4*	*2,1*	*63*
Min Mx	*178*	*-3,2*	*-2,3*	*0*	*-0,4*	*0,6*	*64*
Max My	*185,9*	*-6,2*	*21,6*	*0*	*3,9*	*1,1*	*65*
Min My	*96,8*	*-8,1*	*-2,3*	*0*	*-0,4*	*1,4*	*58*
Max Mz	*137,7*	*-16,9*	*18,8*	*0*	*3,4*	*3*	*61*
Min Mz	*88,6*	*5,9*	*1,5*	*0*	*0,3*	*-1,1*	*49*

Examination of the results in the tables above shows that the main difference is that the loads calculated with Eurocode 1 become higher and for the most congested pile number 66 it is 9 kPa or 5 %.

The data of cross-sectional forces for all 66 piles are presented in the Appendix IV. It should be noted an increasing pressure load on piles 6,12,18,24,30,36,42,48, 54, 65 and 66 at the last row of pile cap which is located furthest away from the embankment.

From the Tables 7.1 and 7.2 it is obvious that the pile number 66 is exposed to the maximum load. This pile will go to the structural failure if capacity of the pile is exceeded. To check if the pile number 66 is not going to structural collapse, a constructive and geotechnical bearing capacity of the pile were analyzed at the end of this chapter.

The results of the maximum load on the pile when the wind load increase due to higher wind velocity of 28 m/s and 30,9 m/s are summarized in Table 7.3 and Table 7.4.

Table 7.3 Max cross-sectional forces v=28 m/s

	Forces (kN)	*Nx*	*Vy*	*Vz*	*Mx*	*My*	*Mz*	*Pile*
BSV97	*Max Nx*	*193,5*	*-3*	*1,4*	*0*	*0,3*	*0,5*	*66*
Eurocode 1	*Max Nx*	*205,1*	*-3,2*	*0,6*	*0*	*0,1*	*0,6*	*66*

Table 7.4 Max cross-sectional forces v=30,9 m/s

	Forces (kN)	*Nx*	*Vy*	*Vz*	*Mx*	*My*	*Mz*	*Pile*
BSV97	*Max Nx*	*204,1*	*-3,2*	*0,7*	*0*	*0,1*	*0,6*	*66*
Eurocode 1	*Max Nx*	*218*	*-3,4*	*-0,3*	*0*	*0,1*	*0,6*	*66*

7.2.2 The load on the piles caused by south wind

The structural capacity of the piles is even calculated for other wind direction. The dominant winds from the south and north could also jeopardize the tower's stability. Below are the results of max load on the pile due to south wind. The tables are summarized for wind velocity of 25, 28 and 30,9 m/s.

Table 7.5 Max cross-sectional forces v=25 m/s

	Forces (kN)	*Nx*	*Vy*	*Vz*	*Mx*	*My*	*Mz*	*Pile*
BSV97	*Max Nx*	*180,3*	*2*	*15,5*	*0*	*2,8*	*-0,4*	*66*
Eurocode 1	*Max Nx*	*179,8*	*2,1*	*15,5*	*0*	*2,8*	*-0,4*	*66*

Table 7.6 Max cross-sectional forces v=28 m/s

	Forces (kN)	*Nx*	*Vy*	*Vz*	*Mx*	*My*	*Mz*	*Pile*
BSV97	*Max Nx*	*186,1*	*2,2*	*15,4*	*0*	*2,8*	*-0,4*	*66*
Eurocode 1	*Max Nx*	*185,5*	*2,4*	*15,4*	*0*	*2,8*	*-0,4*	*66*

Table 7.7 Max cross-sectional forces v=30,9 m/s

	Forces (kN)	*Nx*	*Vy*	*Vz*	*Mx*	*My*	*Mz*	*Pile*
BSV97	*Max Nx*	*192,4*	*2,4*	*15,4*	*0*	*2,7*	*-0,4*	*66*
Eurocode 1	*Max Nx*	*191,6*	*2,6*	*15,3*	*0*	*2,7*	*-0,5*	*66*

7.2.3 The load on the piles caused by north wind

The north wind has the same direction as the horizontal force from the water load i.e. both acting on the east tower in positive (y) direction. Below are the results of max load on a pile due to north wind. The tables are summarized for wind velocity of 25, 28 and 30,9 m/s.

Table 7.8 Max cross-sectional forces v=25 m/s

	Forces (kN)	*Nx*	*Vy*	*Vz*	*Mx*	*My*	*Mz*	*Pile*
BSV97	*Max Nx*	*169,4*	*-1,5*	*5,1*	*0*	*0,9*	*0,3*	*59*
Eurocode 1	*Max Nx*	*168,8*	*-1,4*	*5,1*	*0*	*0,9*	*0,2*	*59*

Table 7.9 Max cross-sectional forces v=28 m/s

	Forces (kN)	*Nx*	*Vy*	*Vz*	*Mx*	*My*	*Mz*	*Pile*
BSV97	*Max Nx*	*175,4*	*-1,4*	*5,2*	*0*	*0,9*	*0,2*	*59*
Eurocode 1	*Max Nx*	*174,8*	*-1,2*	*5,2*	*0*	*0,9*	*0,2*	*59*

Table 7.10 Max cross-sectional forces v=30,9 m/s

	Forces (kN)	*Nx*	*Vy*	*Vz*	*Mx*	*My*	*Mz*	*Pile*
BSV97	*Max Nx*	*182*	*-1,2*	*5,3*	*0*	*0,9*	*0,2*	*59*
Eurocode 1	*Max Nx*	*181,2*	*-1*	*5,3*	*0*	*1*	*0,2*	*59*

A review of all the above results for the east, south and north wind gives more or less consistent results between the two methods with calculations of the maximum normal forces. The largest differential of 5 % is estimated due to the east wind. The difference between shear forces and moment is marginal or none.

7.3 Deformations

Both vertical and transverse deformations are shown in the results below. Shifts are positive, when it is coincide with the directions of the positive coordinate axes. Rotations are positive when they rotate counterclockwise about the axes.

The pile cap deformations are presented in the global coordinate system with origin in the middle of the plate. Rotations and displacements in accordance to BSV97 and Eurocode 1 has presented in tables below for east, south and north wind. Deformations of the pile cap caused by the east wind are presented in Table 7.11.

The analyses of results from the table 7.11, realizes that the vertical and lateral displacement is significant. It corresponds to almost 1,2 cm downward along the x-axis (dx) and between 0,6 and 0,8 cm along the z axis (dz).

This large displacement is caused by the combined effect of the vertical and the horizontal forces. It should be noted that the plate rotations (r) around all three directions is negligible or none.

Table 7.11 Pile cap displacements and rotations at the origin, v=25 m/s

	dx(mm)	*dy(mm)*	*dz(mm)*	*rx(mm)*	*ry(mm)*	*rz (mm)*
BSV97	*11,95*	*0,12*	*6,12*	*0,053*	*0,044*	*0*
Eurocode 1	*11,91*	*0,12*	*6,52*	*0,053*	*0,056*	*0*

Table 7.11 Pile cap displacements and rotations at the origin, v=28 m/s

	dx(mm)	*dy(mm)*	*dz(mm)*	*rx(mm)*	*ry(mm)*	*rz (mm)*
BSV97	*11,91*	*0,12*	*6,56*	*0,053*	*0,057*	*0*
Eurocode 1	*11,85*	*0,12*	*7,08*	*0,053*	*0,073*	*0*

Table 7.11 Pile cap displacements and rotations at the origin, v=30,9 m/s

	dx(mm)	*dy(mm)*	*dz(mm)*	*rx(mm)*	*ry(mm)*	*rz (mm)*
BSV97	*11,86*	*0,12*	*7,05*	*0,053*	*0,072*	*0*
Eurocode 1	*11,80*	*0,12*	*7,67*	*0,053*	*0,091*	*0*

7.3.1 Deformations of pile cap caused by the south and north wind

The trend of the deformations caused by the south wind (upper row of the table) and the north wind (lower row) at the pile cap is shown in the tables below. We see an increase in the deformations along the y-axis and a constant value of 12,12 mm along the x-axis.

Table 7.12 Pile cap displacements and rotations at the origin, v=25 m/s

	dx(mm)	*dy(mm)*	*dz(mm)*	*rx(mm)*	*ry(mm)*	*rz (mm)*
BSV97	*12,12*	*1,11*	*4,37*	*0,054*	*-0,008*	*-0,015*
	12,12	*-0,88*	*4,37*	*0,053*	*-0,008*	*0,014*
Eurocode 1	*12,12*	*1,19*	*4,37*	*0,054*	*-0,008*	*-0,014*
	12,12	*-0,96*	*4,37*	*0,053*	*-0,008*	*0,013*

Table 7.12 Pile cap displacements and rotations at the origin, v=28 m/s

	dx(mm)	*dy(mm)*	*dz(mm)*	*rx(mm)*	*ry(mm)*	*rz (mm)*
BSV97	*12,12*	*1,36*	*4,37*	*0,055*	*-0,008*	*-0,018*
	12,12	*-1,13*	*4,37*	*0,052*	*-0,008*	*0,017*
Eurocode 1	*12,12*	*1,47*	*4,37*	*0,055*	*-0,008*	*-0,017*
	12,12	*-1,23*	*4,37*	*0,052*	*-0,008*	*0,017*

Table 7.12 Pile cap displacements and rotations at the origin, v=30,9 m/s

	dx(mm)	*dy(mm)*	*dz(mm)*	*rx(mm)*	*ry(mm)*	*rz (mm)*
BSV97	*12,12*	*1,64*	*4,37*	*0,055*	*-0,008*	*-0,022*
	12,12	*-1,40*	*4,37*	*0,052*	*-0,008*	*0,021*
Eurocode 1	*12,12*	*1,76*	*4,37*	*0,055*	*-0,008*	*-0,021*
	12,12	*-1,53*	*4,37*	*0,052*	*-0,008*	*0,021*

Detailed results of all piles deformations are shown in Appendix V. It is noteworthy that the piles have more or less constant rotation around all three axes for all piles. The biggest displacement are along x-axis (0,08- 1,6) and z-axis (0,02-1,3) cm in bath cases. A clear trend can be seen that the largest vertical displacement increases toward the plane's edge i.e. those piles with maximum distance from the embankment.

Results of those most displaced piles in both horizontal and vertical direction are shown in Table 7.13.

Tabell 7.13 - The piles with maximum deformation

	BSV 97	*Eurocode 1*	*pile*
dx(mm)	*14,86*	*15,63*	*6*
dy(mm)	*-10,14*	*-10,43*	*61*
dz(mm)	*12,93*	*13,31*	*65*

As shown in the table above, the pile 6 has the maximum vertical offset. The maximum transverse displacement is achieved in the pile 61 along the y-axis and the pile 65 along the z axis. It should be noted that the piles 61, 65 are slanted piles and the pile 6 are vertical. The deformations along all three axes will increase about 5-7% due to wind increase.

7.4 Bearing capacity

7.4.1 Geotechnical bearing capacity

Geotechnical bearing capacity is the capacity of soil to support the loads applied to the ground. The piles are considered as an end-bearing piles trimmed into the bedrock.

Bearing capacity is determined by the rock's resistance. Bedrock in Sweden consists mainly of ancient rocks (e.g. granite and gneiss), whose strength is up to 200 MPa that is much higher than the pile strength. Therefore, pile bearing capacity is limited by the pile's load capacity or constructive resistance. The requirement is that the end-borne piles capacity with regard to fracture in the bedrock verifies by sinking measurement at stop punching (Pile foundations 1993).

Section of an end-bearing pile trimmed into the bedrock is shown in Figure 7.5.

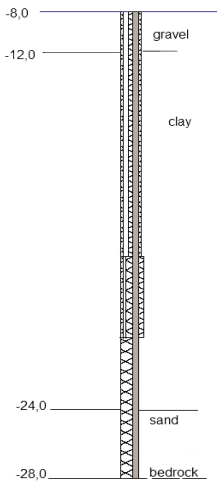

Fig 7.5 – Section of the soil and pile

7.4.2 Structural bearing capacity

Constructive capacity of the pile is the individual pile elements capacity, i.e. its ability to transfer the load effects without collapse or deforms in a damaging way.

The maximum axial stress on a pile is given by equation (7.4).

$$\sigma = \frac{Nx}{A} + \frac{M_r}{W} \qquad (7.4)$$

Mr is the resultant moment of the pile and is given by:

$$M_r = \sqrt{M_y^2 + M_z^2}$$

Substituting the values into equation (7.4) it gives maximum stress on the pile. And for the most congested pile number 66 and in accordance to BSV97 it will be:

$$\sigma_{\max 66} = \frac{183,9}{0,025} + \frac{0,62}{5,7 \cdot 10^{-4}} = 8,4 Mpa$$

The resultant moment for the pile number 66 is:

$$M_r = \sqrt{0,37^2 + 0,5^2} = 0,62 kNm$$

By using the value in accordance to Eurocode 1 we will get some higher stress on the pile.

$$\sigma_{\max 66} = \frac{192,9}{0,025} + \frac{0,58}{5,7 \cdot 10^{-4}} = 8,7 Mpa$$

According to Pile foundation SGI, the capacity of the timber pile (R) can be selected to be 11 MPa provided that the pile consists of fresh round timber with a minimum diameter of 0.13 meter.

By comparing the capacity of timber pile (R) with load effect (S) on the most stressed pile number 66, according to the condition (5.1), it is obvious that the construction is safe.

	BSV 97	Eurocode 1
$R \geq S$	*11 MPa ≥ 8,4 MPa*	*11 MPa ≥ 8,7 MPa*

The tower is stable even in the event of climate change in wind speed i.e. wind speed increases by 12%

11 MPa ≥ 8,8 MPa	*11Mpa ≥ 9,3 Mpa*

Finally the construction are even safe if the instantaneous wind speed of 30.9 m/s strikes the tower from the most critical east side. The load effect is still less than the resistance and the most loaded pile will not go to collapse if calculations are made in according to BSV 97 or Eurocode 1. And since the pile 66 is the most stressed pile all the other piles are also safe.

11MPa≥ 9,2 MPa	*11MPa≥ 9,7 MPa*

8. Conclusion

This master thesis has been studied the effect of permanent and variable loads such as embankment, water- and wind pressure acting on the East Ormo Tower. The effect of the increase in wind speed from different wind directions at the tower's stability has been analyzed using Rymdpålgrupp computer program.

The characteristic and the corresponding design loads is calculated for ultimate limit state and using the partial factor method. Using the software for calculating the stress on piles the author of this master thesis comes to conclusion that the pile 66 is mostly loaded pile. But this load is less than the structural capacity of the pile. Thus the tower is safe against the structural failure, provided that the piles condition is not deteriorated and that the durability of the piles is good enough.

In practice, it is unusual that the wind loads which blows for a relatively shorter time cause failure of construction unless it is extremely high. In this thesis the author had included the maximum increase of 12 % wind up in the region. However the construction will not collapse even if the instantaneous wind speed of 30.9 m/s strikes the tower from the east side. The load effect is still less than the resistance and the most loaded piles will not go to collapse or deforms in a damaging way if calculations are made in according to BSV 97 or Eurocode 1.

Considering the movement, caused by action forces on the tower witch is subjected to both rotation and translation we get significant deformation of the pile cap foundation. The piles have constant rotation around all three axes with lateral displacement along x-axis (0,08-1,6), z-axis (0,02-1,3) and y-axis (0.05-1,0) cm.

The data used in the project were not verified by drilling. There is a lot of information from CPT investigation around the site but no tests were made in connection to tower. The main problem was to identify the thickness and level of both clay and sand layer. Also bedrock slope is an important factor and plays a significant role in determining the carrying capacity of piles. This has not been taken into account in the simplified calculation by hand.

The condition of the wooden pile is also not clearly known. The piles were installed late 1930s and some sort of deterioration should be expected which potentially reduce the strength of the pile.

9. References

Asp, M., Malmsten, S., Återkomsttid vindhastighet, Klimatdata SMHI

Axelsson, M., Bramstång, O., Simonsson, D., (2003), Gasledning Rya-Stenungsund, Beskrivning av utförda stabilitetsundersökningar samt säkerhet utefter ledningssträckningen, SwedPower AB, Gatubolaget Göteborgs Stad, 22pp.

Boverket, 2007, Byggnader i förändrat klimat, Bebyggelsens sårbarhet för klimatförändringarnas och extrema väders påverkan

Bärring, L., Wern, L., (2009): Sveriges vindklimat 1901-2008, Analys av förändring i geostrofisk vind, SMHI 64pp.

Eurocode 1: Action on structures-Part 1-4: General actions-Wind actions, EN 1991-1-4:2005:E

Forsberg, B., Messing, M. L., Jakobsson, B. (2002): {(Ormo skärmanläggning

Fördjupad Dammsäkerhetsutvärdering)}, SwedPower AB,

{P1279200}, Göteborg, {Sweden},124pp.

Gasledning Rya – Stenungsund, Etapp 1- Rya-Guddeby

Beskrivning av utförda stabilitetsundersökningar samt säkerhet utefter ledningssträckningen, SwedPower, Gatubolaget

Handboken bygg, Geoteknik (1984), 603pp.

Holm, G., Olsson, C.(1993), Pålgrundläggning, Statens Geotekniska Institut, 377pp.

Nero, K., Åkerlund S. (1997), Boverkets handbok för snö- och vindlast, BSV 97, 112pp.

Regelsamling för konstruktion (2003) – Boverkets konstruktionsregler, BKR,byggnadsverkslagen och byggnadsverksförordningen 256pp.

Sjöberg, J. (2001): {(Stabilitetsanalys Ormo Skärmanläggning)}, SwedPower AB, {1415600}, Göteborg, {Sweden}, 5pp.

SLIDE, 2D limit equilibrium slope stability verification manual (1989-2006), Rocscience Inc.

Software Engineering, Rymdpålgrupp manual version 1.20.20

Sällförs, G. (2001) – Jordmateriallära, Jordmekanik – Geoteknik, Course Literature

Sällförs, G. (1994) – Slänters Stabilitet, Course Literature

10. Appendixes

Appendix I - Seismic cross section of Ormo screen plant

Appendix II - Site map showing boreholes for CPT tests

Appendix III – The framework and Caisson of the East Ormo Tower

Appendix IV – Cross-Sectional Forces

Appendix V – Deformations

Appendix VI – Variations in Geostrophic wind over southern Sweden, 1901 – 2008, Triangel 1, Göteborg – Visby – Lund and Triangel 2, Göteborg – Stockholm – Visby. (SMHI, Report 138/2009).

Appendix I - Seismic cross section of Ormo screen plant (Ormo skärmanläggning-Fördjupad Dammsäkerhetsutvärdering, SwedPower)

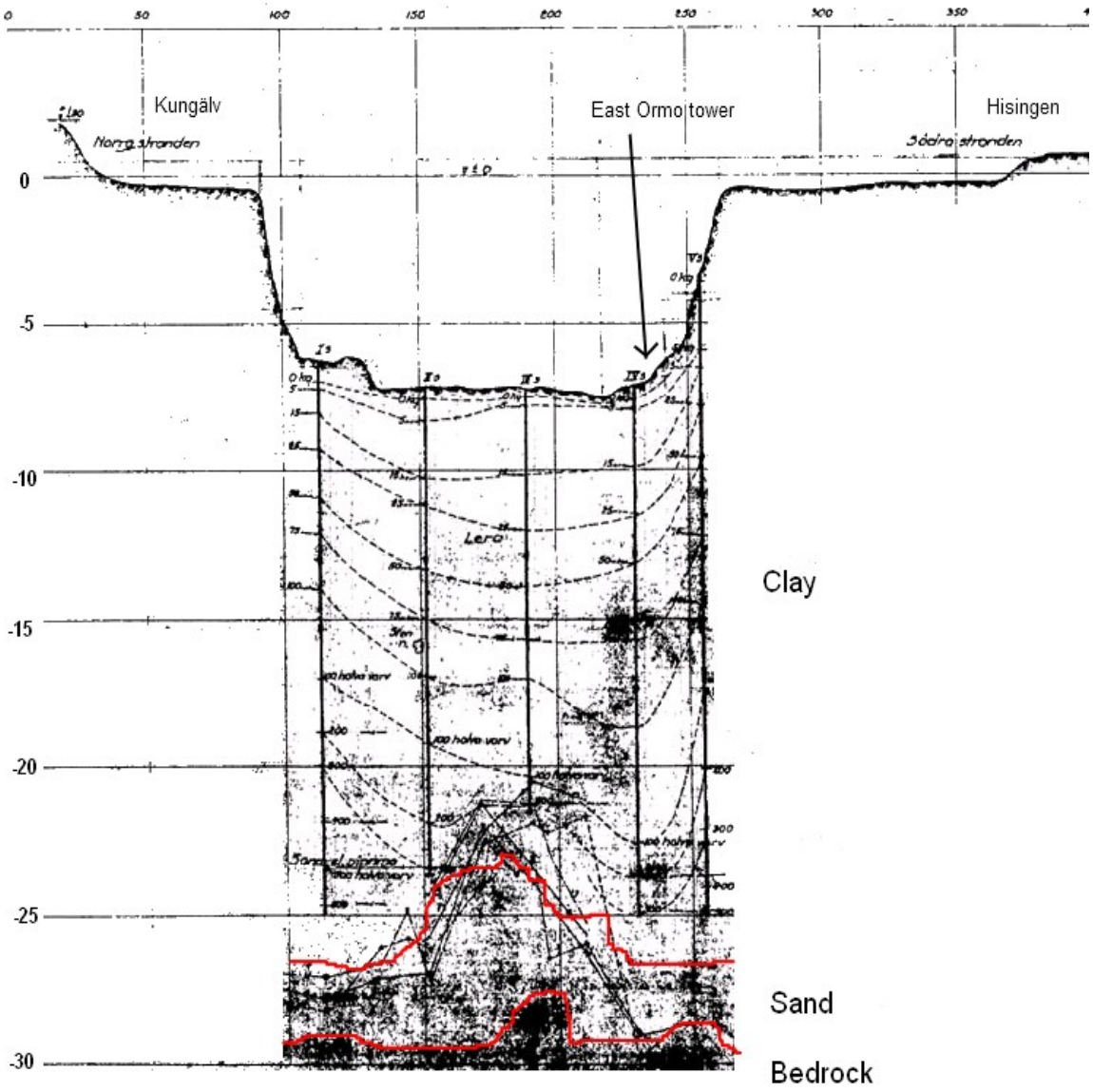

Appendix II - Site map 1:2000 showing boreholes for CPT tests (Gasledning Rya – Stenungsund, SwedPower)

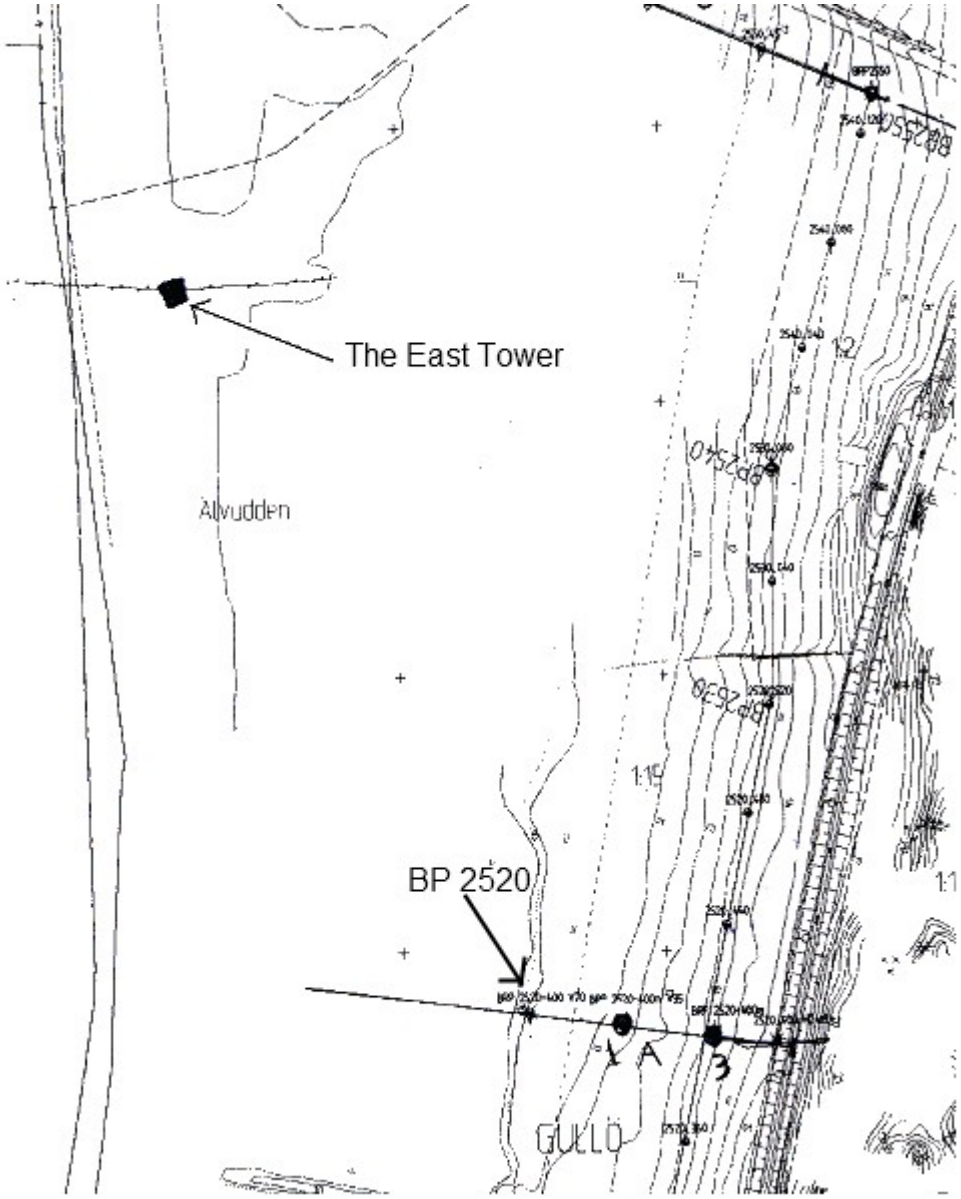

Appendix III – The framework and Caisson of the East Ormo Tower (Ormo skärmanläggning - Fördjupad Dammsäkerhetsutvärdering, SwedPower)

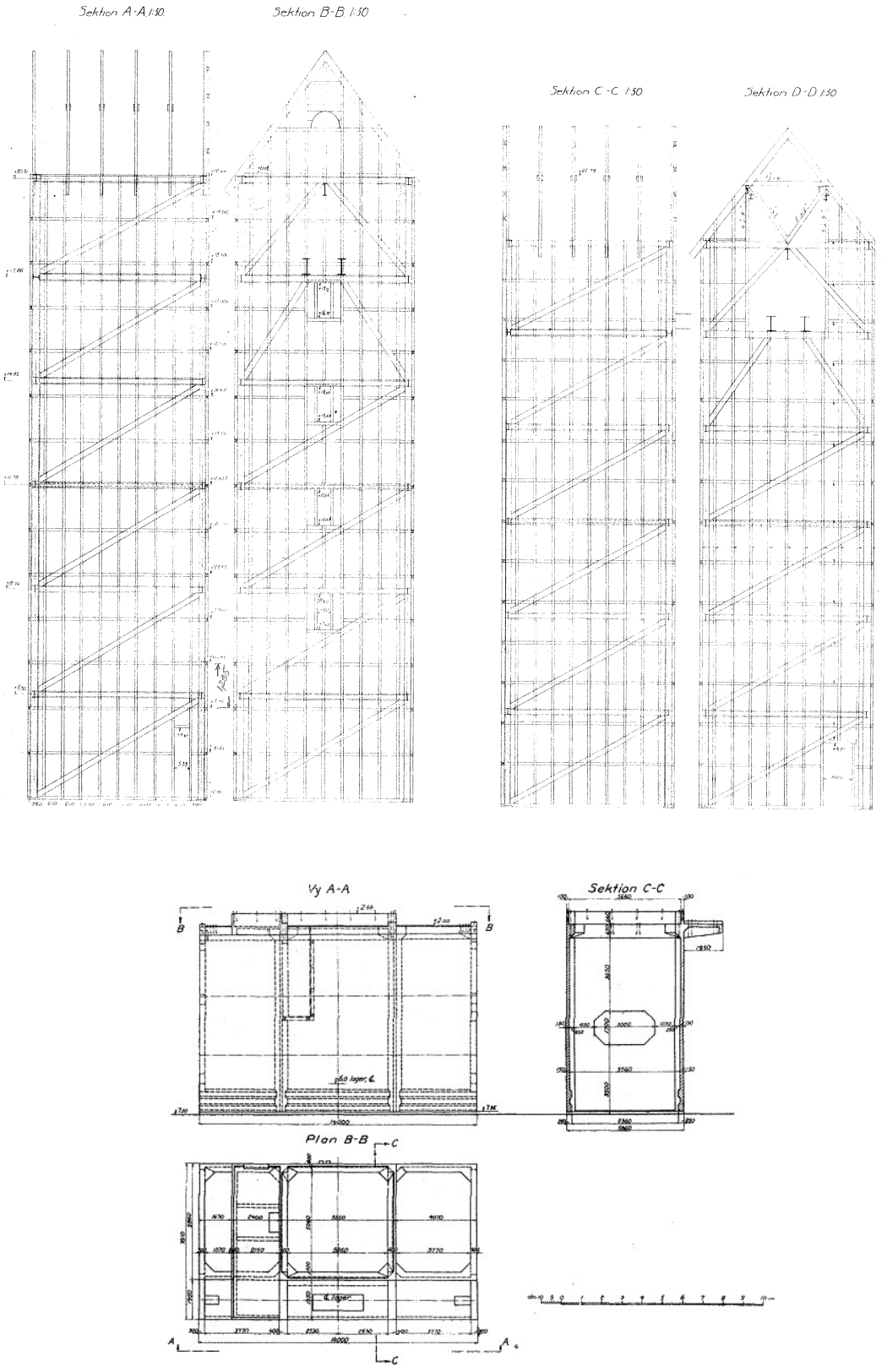

Appendix IV – Cross - sectional forces - BSV97,*v*=25m/s, Rymdpålgrupp

Pile	Nx (kN)	Vy (kN)	Vz (kN)	Mx (kNm)	My (kNm)	Mz (kNm)
1	98.62	5.87	19.02	0.02	3.40	-1.05
2	113.49	3.60	19.02	0.02	3.40	-0.64
3	129.03	1.33	19.02	0.02	3.40	-0.24
4	145.27	-0.95	19.02	0.02	3.40	0.17
5	162.27	-3.22	19.02	0.02	3.40	0.58
6	180.08	-5.49	19.02	0.02	3.40	0.98
7	98.52	5.87	16.75	0.02	3.00	-1.05
8	113.40	3.60	16.75	0.02	3.00	-0.64
9	128.93	1.33	16.75	0.02	3.00	-0.24
10	145.17	-0.95	16.75	0.02	3.00	0.17
11	162.17	-3.22	16.75	0.02	3.00	0.58
12	179.97	-5.49	16.75	0.02	3.00	0.98
13	98.43	5.87	14.48	0.02	2.59	-1.05
14	113.30	3.60	14.48	0.02	2.59	-0.64
15	128.83	1.33	14.48	0.02	2.59	-0.24
16	145.07	-0.95	14.48	0.02	2.59	0.17
17	162.06	-3.22	14.48	0.02	2.59	0.58
18	179.86	-5.49	14.48	0.02	2.59	0.98
19	98.33	5.87	12.21	0.02	2.18	-1.05
20	113.20	3.60	12.21	0.02	2.18	-0.64
21	128.73	1.33	12.21	0.02	2.18	-0.24
22	144.96	-0.95	12.21	0.02	2.18	0.17
23	161.95	-3.22	12.21	0.02	2.18	0.58
24	179.75	-5.49	12.21	0.02	2.18	0.98
25	98.23	5.87	9.94	0.02	1.78	-1.05
26	113.10	3.60	9.94	0.02	1.78	-0.64
27	128.63	1.33	9.94	0.02	1.78	-0.24
28	144.86	-0.95	9.94	0.02	1.78	0.17
29	161.85	-3.22	9.94	0.02	1.78	0.58
30	179.65	-5.49	9.94	0.02	1.78	0.98
31	98.14	5.87	7.66	0.02	1.37	-1.05

Pile	Nx (kN)	Vy (kN)	Vz (kN)	Mx (kNm)	My (kNm)	Mz (kNm)
32	113.00	3.60	7.66	0.02	1.37	-0.64
33	128.53	1.33	7.66	0.02	1.37	-0.24
34	144.76	-0.95	7.66	0.02	1.37	0.17
35	161.74	-3.22	7.66	0.02	1.37	0.58
36	179.54	-5.49	7.66	0.02	1.37	0.98
37	98.04	5.87	5.39	0.02	0.97	-1.05
38	112.90	3.60	5.39	0.02	0.97	-0.64
39	128.42	1.33	5.39	0.02	0.97	-0.24
40	144.65	-0.95	5.39	0.02	0.96	0.17
41	161.64	-3.22	5.39	0.02	0.96	0.58
42	179.43	-5.49	5.39	0.02	0.96	0.98
43	97.94	5.87	3.12	0.02	0.56	-1.05
44	112.80	3.60	3.12	0.02	0.56	-0.64
45	128.32	1.33	3.12	0.02	0.56	-0.24
46	144.55	-0.95	3.12	0.02	0.56	0.17
47	161.53	-3.22	3.12	0.02	0.56	0.58
48	179.32	-5.49	3.12	0.02	0.56	0.98
49	97.85	5.87	0.85	0.02	0.15	-1.05
50	112.70	3.60	0.85	0.02	0.15	-0.64
51	128.22	1.33	0.85	0.02	0.15	-0.24
52	144.45	-0.95	0.85	0.02	0.15	0.17
53	161.43	-3.22	0.85	0.02	0.15	0.58
54	179.21	-5.49	0.85	0.02	0.15	0.98
55	96.48	-7.45	20.62	0.02	3.69	1.33
56	93.42	-8.46	1.72	0.01	0.31	1.51
57	116.46	-2.09	18.27	0.02	3.27	0.37
58	101.90	-8.32	-1.61	0.01	-0.29	1.49
59	140.94	2.96	18.58	0.02	3.33	-0.53
60	114.26	-7.87	-0.32	0.01	-0.06	1.41
61	132.32	-16.47	18.21	0.02	3.26	2.95
62	161.60	-3.39	-0.69	0.01	-0.12	0.61
63	151.43	-11.47	18.27	0.02	3.27	2.05

Pile	Nx (kN)	Vy (kN)	Vz (kN)	Mx (kNm)	My (kNm)	Mz (kNm)
64	170.93	-2.89	-1.61	0.01	-0.29	0.52
65	176.87	-6.06	20.99	0.02	3.76	1.09
66	183.88	-2.81	2.09	0.01	0.37	0.50

Cross-Sectional Forces for all piles -Eurocode 1, *v*=25m/s, Rymdpålgrupp

Pile	Nx (kN)	Vy (kN)	Vz (kN)	Mx (kNm)	My (kNm)	Mz (kNm)
1	89.41	5.87	19.68	0.02	3.52	-1.05
2	107.67	3.60	19.68	0.02	3.52	-0.64
3	126.74	1.33	19.68	0.02	3.52	-0.24
4	146.68	-0.95	19.68	0.02	3.52	0.17
5	167.54	-3.22	19.68	0.02	3.52	0.58
6	189.40	-5.49	19.68	0.02	3.52	0.98
7	89.31	5.87	17.40	0.02	3.11	-1.05
8	107.57	3.60	17.40	0.02	3.11	-0.64
9	126.64	1.33	17.40	0.02	3.11	-0.24
10	146.57	-0.95	17.40	0.02	3.11	0.17
11	167.44	-3.22	17.41	0.02	3.11	0.58
12	189.30	-5.49	17.41	0.02	3.11	0.98
13	89.21	5.87	15.13	0.02	2.71	-1.05
14	107.47	3.60	15.13	0.02	2.71	-0.64
15	126.54	1.33	15.13	0.02	2.71	-0.24
16	146.47	-0.95	15.13	0.02	2.71	0.17
17	167.33	-3.22	15.13	0.02	2.71	0.58
18	189.19	-5.49	15.13	0.02	2.71	0.98
19	89.12	5.87	12.86	0.02	2.30	-1.05
20	107.37	3.60	12.86	0.02	2.30	-0.64
21	126.44	1.33	12.86	0.02	2.30	-0.24
22	146.37	-0.95	12.86	0.02	2.30	0.17
23	167.23	-3.22	12.86	0.02	2.30	0.58
24	189.08	-5.49	12.86	0.02	2.30	0.98
25	89.02	5.87	10.59	0.02	1.90	-1.05
26	107.27	3.60	10.59	0.02	1.90	-0.64

Pile	Nx (kN)	Vy (kN)	Vz (kN)	Mx (kNm)	My (kNm)	Mz (kNm)
27	126.34	1.33	10.59	0.02	1.90	-0.24
28	146.26	-0.95	10.59	0.02	1.89	0.17
29	167.12	-3.22	10.59	0.02	1.89	0.58
30	188.97	-5.49	10.59	0.02	1.89	0.98
31	88.92	5.87	8.32	0.02	1.49	-1.05
32	107.17	3.60	8.32	0.02	1.49	-0.64
33	126.23	1.33	8.32	0.02	1.49	-0.24
34	146.16	-0.95	8.32	0.02	1.49	0.17
35	167.02	-3.22	8.32	0.02	1.49	0.58
36	188.86	-5.49	8.32	0.02	1.49	0.98
37	88.83	5.87	6.04	0.02	1.08	-1.05
38	107.07	3.60	6.04	0.02	1.08	-0.64
39	126.13	1.33	6.04	0.02	1.08	-0.24
40	146.06	-0.95	6.05	0.02	1.08	0.17
41	166.91	-3.22	6.05	0.02	1.08	0.58
42	188.75	-5.49	6.05	0.02	1.08	0.98
43	88.73	5.87	3.77	0.02	0.68	-1.05
44	106.98	3.60	3.77	0.02	0.68	-0.64
45	126.03	1.33	3.77	0.02	0.68	-0.24
46	145.95	-0.95	3.77	0.02	0.68	0.17
47	166.80	-3.22	3.77	0.02	0.68	0.58
48	188.65	-5.49	3.77	0.02	0.68	0.98
49	88.63	5.87	1.50	0.02	0.27	-1.05
50	106.88	3.60	1.50	0.02	0.27	-0.64
51	125.93	1.33	1.50	0.02	0.27	-0.24
52	145.85	-0.95	1.50	0.02	0.27	0.17
53	166.70	-3.22	1.50	0.02	0.27	0.58
54	188.54	-5.49	1.50	0.02	0.27	0.98
55	90.22	-7.35	21.24	0.02	3.80	1.32
56	87.16	-8.36	1.10	0.01	0.20	1.50
57	111.37	-1.85	18.92	0.02	3.39	0.33
58	96.81	-8.08	-2.26	0.01	-0.40	1.45

Pile	Nx (kN)	Vy (kN)	Vz (kN)	Mx (kNm)	My (kNm)	Mz (kNm)
59	137.04	3.34	19.20	0.02	3.44	-0.60
60	110.37	-7.49	-0.94	0.01	-0.17	1.34
61	137.71	-16.93	18.83	0.02	3.37	3.03
62	166.98	-3.85	-1.31	0.01	-0.23	0.69
63	158.49	-11.79	18.92	0.02	3.39	2.11
64	177.99	-3.21	-2.26	0.01	-0.40	0.57
65	185.89	-6.24	21.61	0.02	3.87	1.12
66	192.91	-2.98	1.47	0.01	0.26	0.53

Appendix V – Deformations- BSV 97, *v*=25m/s, Rymdpålgrupp

Pile	dx(mm)	dy(mm)	dz(mm)	rx(grad)	ry(grad)	rz(grad)
1	9.11	3.62	11.72	0.053	0.044	0.000
2	10.26	2.22	11.72	0.053	0.044	0.000
3	11.41	0.82	11.72	0.053	0.044	0.000
4	12.56	-0.58	11.72	0.053	0.044	0.000
5	13.71	-1.98	11.72	0.053	0.044	0.000
6	14.86	-3.38	11.72	0.053	0.044	0.000
7	9.10	3.62	10.32	0.053	0.044	0.000
8	10.25	2.22	10.32	0.053	0.044	0.000
9	11.40	0.82	10.32	0.053	0.044	0.000
10	12.55	-0.58	10.32	0.053	0.044	0.000
11	13.70	-1.98	10.32	0.053	0.044	0.000
12	14.85	-3.38	10.32	0.053	0.044	0.000
13	9.09	3.62	8.92	0.053	0.044	0.000
14	10.24	2.22	8.92	0.053	0.044	0.000
15	11.39	0.82	8.92	0.053	0.044	0.000
16	12.54	-0.58	8.92	0.053	0.044	0.000
17	13.69	-1.98	8.92	0.053	0.044	0.000
18	14.84	-3.38	8.92	0.053	0.044	0.000
19	9.08	3.62	7.52	0.053	0.044	0.000
20	10.23	2.22	7.52	0.053	0.044	0.000
21	11.38	0.82	7.52	0.053	0.044	0.000
22	12.53	-0.58	7.52	0.053	0.044	0.000
23	13.68	-1.98	7.52	0.053	0.044	0.000
24	14.83	-3.38	7.52	0.053	0.044	0.000
25	9.07	3.62	6.12	0.053	0.044	0.000
26	10.22	2.22	6.12	0.053	0.044	0.000
27	11.37	0.82	6.12	0.053	0.044	0.000
28	12.52	-0.58	6.12	0.053	0.044	0.000
29	13.67	-1.98	6.12	0.053	0.044	0.000
30	14.83	-3.38	6.12	0.053	0.044	0.000
31	9.06	3.62	4.72	0.053	0.044	0.000

Pile	dx(mm)	dy(mm)	dz(mm)	rx(grad)	ry(grad)	rz(grad)
32	10.21	2.22	4.72	0.053	0.044	0.000
33	11.36	0.82	4.72	0.053	0.044	0.000
34	12.51	-0.58	4.72	0.053	0.044	0.000
35	13.67	-1.98	4.72	0.053	0.044	0.000
36	14.82	-3.38	4.72	0.053	0.044	0.000
37	9.05	3.62	3.32	0.053	0.044	0.000
38	10.20	2.22	3.32	0.053	0.044	0.000
39	11.36	0.82	3.32	0.053	0.044	0.000
40	12.51	-0.58	3.32	0.053	0.044	0.000
41	13.66	-1.98	3.32	0.053	0.044	0.000
42	14.81	-3.38	3.32	0.053	0.044	0.000
43	9.04	3.62	1.92	0.053	0.044	0.000
44	10.20	2.22	1.92	0.053	0.044	0.000
45	11.35	0.82	1.92	0.053	0.044	0.000
46	12.50	-0.58	1.92	0.053	0.044	0.000
47	13.65	-1.98	1.92	0.053	0.044	0.000
48	14.80	-3.38	1.92	0.053	0.044	0.000
49	9.04	3.62	0.52	0.053	0.044	0.000
50	10.19	2.22	0.52	0.053	0.044	0.000
51	11.34	0.82	0.52	0.053	0.044	0.000
52	12.49	-0.58	0.52	0.053	0.044	0.000
53	13.64	-1.98	0.52	0.053	0.044	0.000
54	14.79	-3.38	0.52	0.053	0.044	0.000
55	9.10	-4.59	12.70	0.064	0.023	0.013
56	8.81	-5.21	1.06	0.038	-0.056	0.014
57	10.53	-1.29	11.25	0.064	0.025	0.000
58	9.21	-5.13	-0.99	0.037	-0.058	0.000
59	11.91	1.82	11.45	0.064	0.023	-0.014
60	9.65	-4.85	-0.20	0.038	-0.056	-0.013
61	11.44	-10.14	11.22	0.064	0.023	0.013
62	13.97	-2.09	-0.42	0.038	-0.056	0.014
63	12.79	-7.07	11.25	0.064	0.025	0.000

Pile	dx(mm)	dy(mm)	dz(mm)	rx(grad)	ry(grad)	rz(grad)
64	14.44	-1.78	-0.99	0.037	-0.058	0.000
65	14.25	-3.74	12.93	0.064	0.023	-0.014
66	14.81	-1.73	1.29	0.038	-0.056	-0.013

Deformations -Eurocode 1, *v*=25m/s, Rymdpålgrupp

Pile	dx(mm)	dy(mm)	dz(mm)	rx(grad)	ry(grad)	rz(grad)
1	8.26	3.62	12.12	0.053	0.056	0.000
2	9.73	2.22	12.12	0.053	0.056	0.000
3	11.21	0.82	12.12	0.053	0.056	0.000
4	12.68	-0.58	12.12	0.053	0.056	0.000
5	14.16	-1.98	12.12	0.053	0.056	0.000
6	15.63	-3.38	12.12	0.053	0.056	0.000
7	8.25	3.62	10.72	0.053	0.056	0.000
8	9.72	2.22	10.72	0.053	0.056	0.000
9	11.20	0.82	10.72	0.053	0.056	0.000
10	12.67	-0.58	10.72	0.053	0.056	0.000
11	14.15	-1.98	10.72	0.053	0.056	0.000
12	15.62	-3.38	10.72	0.053	0.056	0.000
13	8.24	3.62	9.32	0.053	0.056	0.000
14	9.71	2.22	9.32	0.053	0.056	0.000
15	11.19	0.82	9.32	0.053	0.056	0.000
16	12.66	-0.58	9.32	0.053	0.056	0.000
17	14.14	-1.98	9.32	0.053	0.056	0.000
18	15.61	-3.38	9.32	0.053	0.056	0.000
19	8.23	3.62	7.92	0.053	0.056	0.000
20	9.70	2.22	7.92	0.053	0.056	0.000
21	11.18	0.82	7.92	0.053	0.056	0.000
22	12.65	-0.58	7.92	0.053	0.056	0.000
23	14.13	-1.98	7.92	0.053	0.056	0.000
24	15.60	-3.38	7.92	0.053	0.056	0.000
25	8.22	3.62	6.52	0.053	0.056	0.000
26	9.70	2.22	6.52	0.053	0.056	0.000

Pile	dx(mm)	dy(mm)	dz(mm)	rx(grad)	ry(grad)	rz(grad)
27	11.17	0.82	6.52	0.053	0.056	0.000
28	12.65	-0.58	6.52	0.053	0.056	0.000
29	14.12	-1.98	6.52	0.053	0.056	0.000
30	15.59	-3.38	6.52	0.053	0.056	0.000
31	8.21	3.62	5.12	0.053	0.056	0.000
32	9.69	2.22	5.12	0.053	0.056	0.000
33	11.16	0.82	5.12	0.053	0.056	0.000
34	12.64	-0.58	5.12	0.053	0.056	0.000
35	14.11	-1.98	5.12	0.053	0.056	0.000
36	15.59	-3.38	5.12	0.053	0.056	0.000
37	8.20	3.62	3.72	0.053	0.056	0.000
38	9.68	2.22	3.72	0.053	0.056	0.000
39	11.15	0.82	3.72	0.053	0.056	0.000
40	12.63	-0.58	3.72	0.053	0.056	0.000
41	14.10	-1.98	3.72	0.053	0.056	0.000
42	15.58	-3.38	3.72	0.053	0.056	0.000
43	8.19	3.62	2.32	0.053	0.056	0.000
44	9.67	2.22	2.32	0.053	0.056	0.000
45	11.14	0.82	2.32	0.053	0.056	0.000
46	12.62	-0.58	2.32	0.053	0.056	0.000
47	14.09	-1.98	2.32	0.053	0.056	0.000
48	15.57	-3.38	2.32	0.053	0.056	0.000
49	8.19	3.62	0.92	0.053	0.056	0.000
50	9.66	2.22	0.92	0.053	0.056	0.000
51	11.13	0.82	0.92	0.053	0.056	0.000
52	12.61	-0.58	0.92	0.053	0.056	0.000
53	14.08	-1.98	0.92	0.053	0.056	0.000
54	15.56	-3.38	0.92	0.053	0.056	0.000
55	8.51	-4.53	13.08	0.067	0.035	0.017
56	8.22	-5.15	0.68	0.034	-0.067	0.018
57	10.07	-1.14	11.66	0.068	0.037	0.000
58	8.75	-4.98	-1.39	0.033	-0.070	0.000

Pile	dx(mm)	dy(mm)	dz(mm)	rx(grad)	ry(grad)	rz(grad)
59	11.58	2.06	11.83	0.067	0.034	-0.018
60	9.33	-4.61	-0.58	0.034	-0.068	-0.017
61	11.91	-10.43	11.60	0.067	0.035	0.017
62	14.44	-2.37	-0.81	0.034	-0.067	0.018
63	13.39	-7.26	11.66	0.068	0.037	0.000
64	15.04	-1.98	-1.39	0.033	-0.070	0.000
65	14.98	-3.84	13.31	0.067	0.034	-0.018
66	15.54	-1.84	0.90	0.034	-0.068	-0.017

Appendix VI - Variations in Geostrophic wind over southern Sweden, 1991 – 2008 (SMHI, Report 138/2009), Triangel 2, Göteborg – Stockholm – Visby.

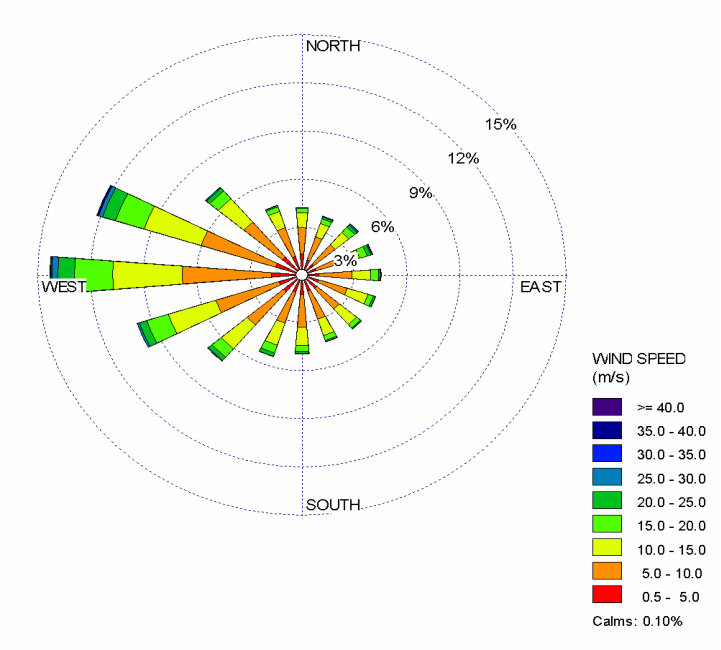

The wind rose for the triangle 2, Gothenburg - Stockholm - Visby

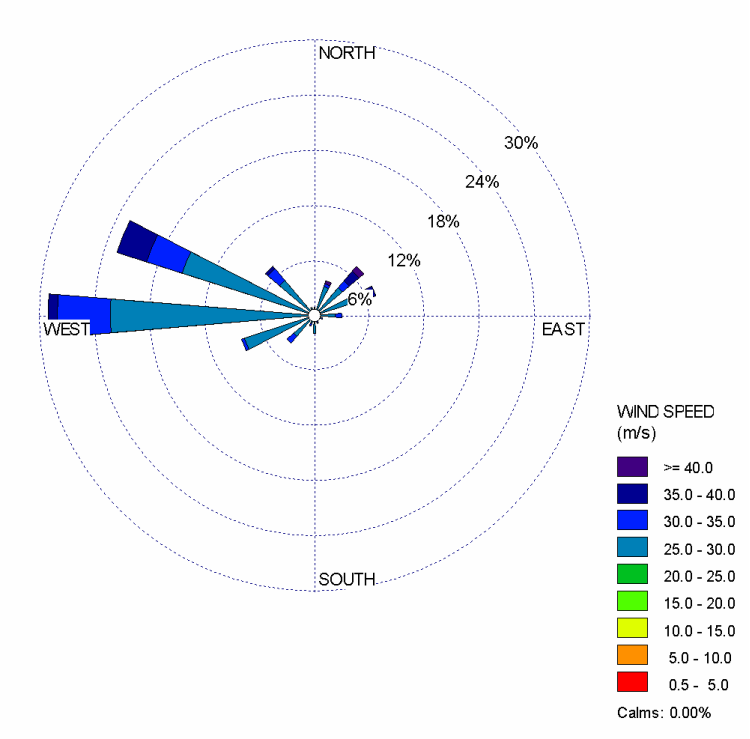

The wind rose for the triangle 2, Gothenburg - Stockholm - Visby when the wind speed is at least 25 m/s